Referee general comment: *really liked reading this paper. The analyses are well thought out and compelling. I think this paper would benefit from a brief overview of the current biogeography/vegetation in the Study Area section. Most of my feedback is regarding the Discussion section and essentially boils down to 'describe the proxy evidence'. Throughout the discussion, the authors keep referencing proxy data, but there is no actual discussion of what that data is. I noted below that they do well with this in lines 556-560 (when they stated that the changes in sedimentology were what suggested the gradual drier conditions), they just need to do it throughout section 5.3. Finally, the paper begins with this idea that large scale climate features have local impacts, and I think the authors should return to that in the conclusion with some brief commentary about how this work is furthering our understanding of local climate, which could have implications on local populations in the future. I also make a few notes about a few minor changes that could be made for the figures.*

We thank the Anonymous Referee #1 for the constructive feedbacks. To address the Referee's comments, we added an overview of the vegetation in the study area, described more thoroughly the proxies existing along Chile and expanded the conclusion to further highlight the importance of large-scale atmospheric pathways on local climate. All additional comments were addressed in the attached document point by point.

This document is built as follow:

- The comments of the Referee are indicated in italic
- Our answers are indicated in normal or bold fonts with bullet points. Modifications to the manuscript are indicated in bold in the tables.

Abstract

0.a.Antarctic cold reversal – consider adding a date to this, just for consistency with the rest of the abstract where you do include dates // 0.b. The abstract is pretty wordy, you could consider rephrasing to something like "We present a leaf-wax reconstruction which reveals distinct dry and wet phases and imply that the drivers of these phases are periodic migrations of the sww belt. From 17-11.5ka, these migrations appear to be tied to changes in the interhemispheric temperature gradient and subsequent changes in Hadley circulation, while the migrations in the Holocene (11.5ka-present) appear to be predominantly controlled by ENSO and insolation."

- The abstract was reformulated as follow:

Old version Ln 16-22	Updates
[…] Here, we use the hydrogen isotope ratios of leaf-wax n-alkanes in marine sediments between 33°S and 36°S offshore Chile to reconstruct past hydrological regimes and the evolution of the SWW belt since the Last Glacial Maximum (LGM, ca. 20,000 cal yr BP). Our results suggest overall wet conditions during the LGM, followed by increasing aridity during the deglaciation period. This shift toward drier conditions was briefly interrupted during the Antarctic Cold Reversal. The early Holocene was then marked by dry conditions until ca. 7,500 yr BP, after which a return to wetter conditions marked latitudes south of 36°S. During the last 5,500 years, wetter conditions progressively characterized latitudes as far north as 30°S. These	[…] Here, we use the hydrogen isotope ratios of leaf-wax n-alkanes in marine sediments between 33°S and 36°S offshore Chile to reconstruct past hydrological regimes and the evolution of the SWW belt since the Last Glacial Maximum (LGM, ca. 20,000 cal yr BP). **Our results reveal distinct dry and wet phases caused by the past latitudinal migration of the SWW belt – with wetter intervals associated with a northerly SWW belt and drier intervals associated with a southerly SWW belt. Our findings imply a northward position of the SWW belt during the LGM, followed by a southward migration of the SWW belt during the deglaciation period. This shift southward was briefly interrupted during the Antarctic Cold**

results reflect past changes in the latitudes of the SWW belt and imply a northward position of the SWW belt during the LGM, followed by a southward migration of the SWW belt during the deglaciation period. This shift southward was briefly interrupted during the Antarctic Cold Reversal. The SWW belt reached its southernmost latitudes during the early Holocene. At ca. 7,500 yr BP, a displacement northward of the SWW belt was detected at latitudes south of 36°S and during the last 5,500 years, the SWW belt progressively migrated northward. Our reconstruction, compared with past latitude of the ITCZ, shows that the climate was predominantly, but not exclusively, controlled by the El-Niño Southern Oscillation and insolation during the Holocene, while atmospheric pathways associated with large interhemispheric temperature gradient and changes in the Hadley cell circulation prevailed from 17,000 to 11,500 cal yr BP.	**Reversal (ca. 14,700 to 13,000 cal yr BP). The SWW belt reached its southernmost latitudes during the early Holocene. At ca. 7,500 yr BP, a displacement northward of the SWW belt was detected at latitudes south of 36°S and, during the last 5,500 years, the SWW belt progressively migrated northward. From 17,000 to 11,500 cal yr BP, these migrations appear to be tied to atmospheric circulation regimes resulting from large changes in the interhemispheric temperature gradient and subsequent changes in the Hadley cell circulation, while the migrations in the Holocene (11,500 cal yr BP to present) appear to be predominantly controlled by insolation and atmospheric circulation regimes resembling those of El-Niño Southern Oscillation events.**

Introduction

1.a.i Intro sentence sets this up to be 'large scale climate features have local impacts', how does your first example impact local climate -- Consider adding some mention of how shifts in the sww belt impact the westerly storm track, winter rainfall, etc.

- The manuscript was reformulated as follow. Note that this answer also encompasses the answer to the comment of Anonymous Referee #2 concerning defining the "modern components" of the SWW and the ITCZ.

Old Ln. 38-42	New
[…] moisture and heat both intra- and interhemispherically (e.g., Hadley, 1997; Watt-Meyer and Frierson, 2019). The modern components of the SWW are relatively well understood (e.g., Garreaud, 2009; Garreaud et al., 2009) and several studies have investigated their past evolution (e.g., Arbuszewski et al., 2013; Haug et al., 2001; Kaiser et al., 2024; Lamy et al., 2001; Sachs et al., 2009), yet forcing mechanisms and especially dynamic feedbacks between these systems remain debated.	[…] moisture and heat both intra- and interhemispherically (e.g., Hadley, 1997; Watt-Meyer and Frierson, 2019). **Furthermore, these climate systems strongly affect regional climate. For instance, the seasonal changes in the latitude of the SWW belt determine precipitation regimes in central Chile (Garreaud et al., 2009).** The modern components of the SWW and the ITCZ **– that is seasonal changes in their position and/or their response to climate phenomena such as the El Niño–Southern Oscillation (ENSO) –** are relatively well understood (e.g., Garreaud, 2009; Garreaud et al., 2009) and several studies have investigated their past evolution **(e.g., Arbuszewski et al., 2013; Haug et al., 2001; Kaiser et al., 2024; Lamy et al., 2001; Mohtadi et al., 2004; Sachs et al., 2009),** yet forcing mechanisms and especially dynamic feedbacks between these systems remain debated.

1.b. Line 49-50: previous sentence says the issue is the lack of high-res reconstructions, so I'd modify this sentence to be "Here we aim… by generating several high-resolution hydroclimate records."

Old Ln. 49-50	New
Here, we aim to investigate the atmospheric pathways acting on the west coast of South America and, thus, the Southern Hemisphere (SH) since the LGM.	Here, we aim to investigate the atmospheric pathways acting on the west coast of South America and, thus, the Southern Hemisphere (SH) since the LGM **by generating high-resolution hydroclimate records**.

1.c.d. Line 65: "drier conditions were inferred" → inferred from what kind of record? -- Lines 67-69: same thing as above, what kind of evidence or records support those inferences? Paleobotanical? Geochemical?

Old Ln. 65-69	New
For instance, increasingly drier conditions were inferred between 13.5 and 11.5 ka BP at the latitude of 30°S (Bernhardt et al., 2017; Kaiser et al., 2024), while wetter conditions marked this period at the latitude of 34°S (Valero-Garcés et al., 2005). Several records also supported drier conditions along Chile between ca. 11 and 7 ka BP (Jara and Moreno, 2014; Jenny et al., 2002a), while some high-altitude records indicated increases in relative moisture during the same time period (e.g., Fiers et al., 2019; de Porras et al., 2014).	For instance, increasingly drier conditions were inferred **from organic biomarker record and a humidity index record derived from grain-size distribution** between 13.5 and 11.5 ka BP at the latitude of 30°**S (site GeoB7139-2, Bernhardt et al., 2017; Kaiser et al., 2024)**, while wetter conditions, inferred **from lake sediment archives and pollen assemblages** marked this period at the latitude of 34°S (Valero-Garcés et al., 2005). Several **palaeobotanical, charcoal and sedimentary** records also supported drier conditions along Chile between ca. 11 and 7 ka BP (Jara and Moreno, 2014; Jenny et al., 2002a), while some high-altitude **pollen, charcoal and geochemical records** indicated increases in relative moisture during the same time period (e.g., Fiers et al., 2019; de Porras et al., 2014).

1.e. Overall, I think the intro is good, but it does read as a little bit scattered, the purpose of each paragraph could be more clearly defined Paragraph 1: large scale systems impact local climate, here's examples of large scale features and how they impact local climate in modern, we don't know about the past . paragraph 2: previous studies lack resolution of sww belt to clearly elucidate how large scale impacts small scale in the past, we want to do that using sediment from west coast of south America. paragraph 3: here's why the study region is ideal for this . paragraph 4: here's the tool we're using for this.

- The main structure of the introduction was not changed as we consider that the structure of our paragraphs helps emphasizing the final output of this study, which is identifying atmospheric pathways:
    - Paragraph 1 (global scale): Why studying the evolution of the SWW /SPH and ITCZ matters and which mechanisms associated with these features still lack constraints?
    - Paragraph 2 (global scale): Why atmospheric pathways acting at global scale are still not identified? Lack of combined high-resolution reconstructions of the evolution of the SWW belt and the ITCZ during the same time period.

- Paragraph 3 (west coast of South America): Spatial focus of this study: why is the west coast of South America an ideal site to study atmospheric pathways?
- Paragraph 4 (west coast of South America): temporal focus of this study: which time period is studied and which information is lacking during this time period to identify atmospheric pathways.
- Paragraph 5: Our approach to tackle this issue. (Note that the previous paragraph 5 and 6 were now combined in a single paragraph).

- In order to facilitate the readability of the Introduction and emphasize the importance of circulation regimes on local climate, the following modifications were however performed:

Old Ln. 38-39	New
[…] moisture and heat both intra- and interhemispherically (e.g., Hadley, 1997; Watt-Meyer and Frierson, 2019).	[…] moisture and heat both intra- and interhemispherically (e.g., Hadley, 1997; Watt-Meyer and Frierson, 2019). **Furthermore, these climate systems strongly affect regional climate. For instance, the seasonal changes in the latitude of the SWW belt determine precipitation regimes in central Chile (Garreaud et al., 2009). [see answer comment 1.a.i]**
The ascent of moisture-laden air masses from the westerlies' storm track along the Andes generates orographic precipitations in Central and Southern Chile (e.g., Barrett et al., 2009; Garreaud, 2009). Any changes in the position or structure of these climate features caused by changes in atmospheric pathways should thus be translated by hydroclimate changes in South America. Reconstructing hydrological regimes along the west coast of South America can thus shed light on the past connections between these large-scale atmospheric features. (Ln. 56-60)	The ascent of moisture-laden air masses from the westerlies' storm track along the Andes generates orographic precipitations in Central and Southern Chile (e.g., Barrett et al., 2009; Garreaud, 2009). **Any changes in the position or structure of these climate features, resulting from different atmospheric pathways, should thus be recognizable by changes in regional hydroclimate. High-resolution spatial and temporal reconstructions of hydroclimate along the west coast of South America can thus help shedding lights on past atmospheric pathways.**
The last 20 kyr were characterized by major climate changes in South America, such as the Glacial-Interglacial transition. (Ln. 61)	**Here, we focus on the last 20 kyr as this period was** characterized by major climate changes, such as the Glacial-Interglacial transition.
Specifically, we reconstruct the past extent of SPH- and SWW-driven moisture and use this new reconstruction to investigate the atmospheric pathways acting on the South American climate since the LGM. (Ln. 86-88)	Specifically, we reconstruct the past extent of SPH- and SWW-driven moisture **based on past changes in regional hydroclimate along Chile** and use this new reconstruction to investigate the atmospheric pathways acting on the South American climate since the LGM.
Previous paragraphs 5 and 6 were combined in a single paragraph (Ln. 73-88)	

Study area

2.a.i and ii Line 113: I would just add the word leaf-wax here. ("use it to calibrate the leaf-wax signal recorded in marine archives.") -- Also, what do you mean by calibrate? Is there an actual mathematical calibration you're using or do you mean that you're using the Gaviria-Lugo record to aid your interpretation of the paleorecord?

- We are using the Gaviria-Lugo record to aid our interpretation. The manuscript was thus modified as follows:

Old (Ln. 113)	New
We therefore consider the signal of modern fluvial sediments recorded by Gaviria-Lugo et al. (2023a, b) as representative of continental conditions and use it to calibrate the signal recorded in marine archives.	We therefore consider the signal of modern fluvial sediments recorded by Gaviria-Lugo et al. (2023a, b) as representative of continental conditions and use it to **interpret** the **leaf-wax** signal recorded in marine archives.

2.a.iii See my note about Figure 1below –

- As Figure 1 was already full of information, we decided to indicate the source area of sites GeoB7139-2, GeoB3304-5 and 22SL in Figure S8 as suggested by the Referee. Figure S8 (and its caption) was modified as follows and renamed into Figure S2 (previous Figures S2 to S7 were renamed accordingly).

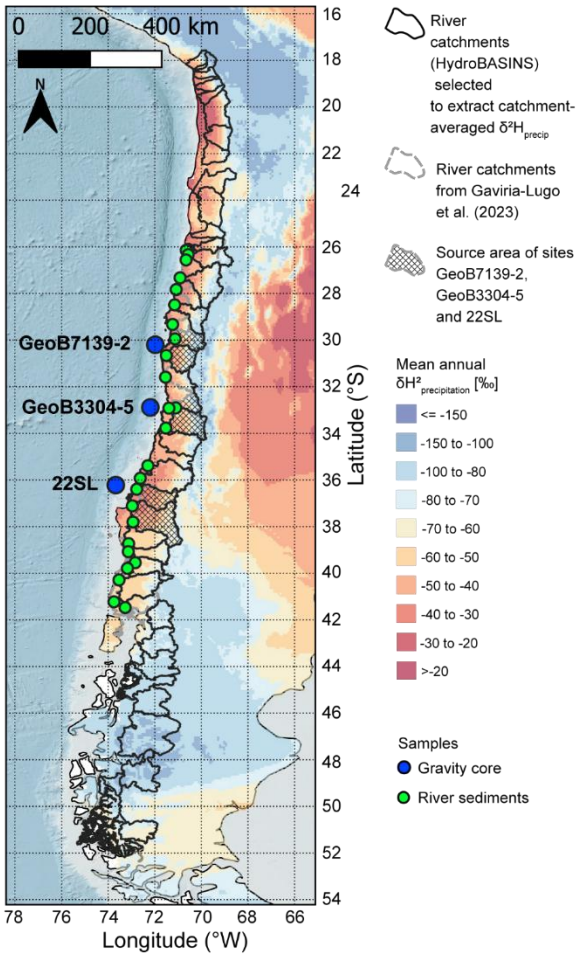

Figure S2. Catchment contours of the HydroBASINS Level 6 map (Hydroshed, Lehner et al., 2006; Lehner and Grill, 2013) compared with the catchment contours from Gaviria-Lugo et al. (2023a) with sampling sites. Fluvial sediments (green), and gravity cores (dark blue). Mean annual δ^2H_{precip} map (Bowen et al., 2005; Bowen and Revenaugh, 2003; Waterisotopes Database, 2017). HydroBASINS map accessed the 27.03.2025. **The source areas of sites GeoB7139-2, GeoB3304-5 and 22SL are indicated by the diamond line pattern. These consist in the catchments of the Elqui, Limari, Aconcagua, Maipo, Itata and Biobío rivers listed from North to South.**

- References to Fig.S2 were also added to the manuscript.

Old (Ln. 118-126)	New
We selected two sediment gravity cores to reconstruct past hydrological changes (Fig. 1). At 33°S, core GeoB3304-5 (32.89°S-72.19°W, R/V Sonne Cruise SO102, Hebbeln and Shipboard Scientists, 1995) comprises sediments transported by the Maipo and the Aconcagua Rivers. At 36°S near the mouth of the Biobío and the Itata Rivers, we selected core 22SL (36.22°S - 73-68°W, Sonne Cruise SO161-5, Wiedicke-Hombach and Shipboard Scientific Party, 2002). To extend the latitudinal coverage of this study, we combined these two records with the published δ^2H_{wax} record of site GeoB7139-2 (30.20°S-71.98°W, R/V Sonne Cruise SO156, Hebbeln and Shipboard Scientists, 2001) from Kaiser et al. (2024). We also report new radiocarbon ages for these three sites. From a sedimentological point of view, site GeoB7139-2, located near the mouth of the Elqui and Limarí Rivers, closely resembles that of sites GeoB3304-5 and 22SL with source areas extending from the Pacific coast to the high Andes.	We selected two sediment gravity cores to reconstruct past hydrological changes (Fig. 1). At 33°S, core GeoB3304-5 (32.89°S-72.19°W, R/V Sonne Cruise SO102, Hebbeln and Shipboard Scientists, 1995) comprises sediments transported by the Maipo and the Aconcagua Rivers **(Fig. S2 in Supplementary Material)**. At 36°S near the mouth of the Biobío and the Itata Rivers **(Fig. S2 in Supplementary Material)**, we selected core 22SL (36.22°S - 73-68°W, Sonne Cruise SO161-5, Wiedicke-Hombach and Shipboard Scientific Party, 2002). To extend the latitudinal coverage of this study, we combined these two records with the published δ^2H_{wax} record of site GeoB7139-2 (30.20°S-71.98°W, R/V Sonne Cruise SO156, Hebbeln and Shipboard Scientists, 2001) from Kaiser et al. (2024). We also report new radiocarbon ages for these three sites. From a sedimentological point of view, site GeoB7139-2, located near the mouth of the Elqui and Limarí Rivers **(Fig. S2 in Supplementary Material)**, closely resembles that of sites GeoB3304-5 and 22SL with source areas extending from the Pacific coast to the high Andes.

2.a.iv is there any potential for aeolian deposition of waxes into the sediment, or do the local wind patterns not facilitate this?

- We consider that the aeolian deposition of waxes unlikely at the latitudes of the gravity cores due to the predominant influence of the eastward-blowing westerly winds at these latitudes.

Old (Ln. 109-110)	New
Aeolian transport of sediments – occurring today in the hyper-arid to arid regions of northern Chile – was likely minor south of 33°S during the last 20 kyr (Lamy et al., 1998; Stuut et al., 2007; Stuut and Lamy, 2004). We therefore consider	Aeolian transport of sediments – occurring today in the hyper-arid to arid regions of northern Chile – was likely minor south of 33°S during the last 20 kyr (Lamy et al., 1998; Stuut et al., 2007; Stuut and Lamy, 2004). **This implies low levels of aeolian deposition of wax at the at the latitudes of the gravity cores further supported by the influence of the eastward-blowing westerly winds at these latitudes (Lamy et al., 2001; Montade et al., 2011).** We therefore consider […]

2.b.i CLIMATE FEATURES AND TEMPORAL PATTERNS ALONG THE WEST COAST OF SOUTH AMERICA I really like this section, I think it is well written and describes regional climate very well, however I do think it could use a description of the overall biogeography of Chile. What biomes are present, what's the dominant vegetation of each biome, etc.

- A section was added to the manuscript presenting modern vegetation as well as a brief overview of past vegetation changes.

New section:

2.3 Present and past vegetation along Chile

Chile is marked by highly heterogenous vegetation with vegetation ranging from plant assemblages typical of hyper arid conditions in the north, such as semi-desert scrubs and grasslands, to plant assemblages typical of hyper humid conditions in the south, such as montane evergreen forests (e.g., Luebert and Pliscoff, 2022). Here we focus on describing the dominant macrogroups defined by Luebert and Pliscoff (2022) between the latitudes of 26°S and 42°S. Further details on high altitude vegetation or macrogroups occurring in coastal areas can be found in Luebert and Pliscoff (Luebert and Pliscoff, 2022).

At present, the *Chilean Mediterranean Interior Semi-Desert Scrub & Grassland* macrogroup prevails between the latitude of 26°S and ca. 32°S (Luebert and Pliscoff, 2022). This macrogroup is composed of drought-resistant plant assemblages and is mainly associated with punctual orogenic precipitation and/or fogs in coastal areas (e.g., Garreaud et al., 2001, 2008). Toward the south, ecosystems typical of Mediterranean vegetation develop with increasing winter precipitation. These includes the *Central Chilean Interior Scrub* and *Chilean Mediterranean Sclerophyllous Forest* macrogroups found between ca. 32°S and 38°S. Further south, these macrogroups are replaced by the *Chilean Mediterranean Deciduous Forest* (ca. 35°S to 39°S) identified by the presence of *Nothofagus obliqua* (e.g., Heusser, 2003) and characteristic of more humid conditions (Fig. 1a, Luebert and Pliscoff, 2022). South of 37°S, Mediterranean vegetation is replaced by the *Valdivian Lower Montane Deciduous Forest* macrogroup occurring between ca. 37°S to 42°S and the *Valdivian Lower Montane Evergreen Forest* macrogroup occurring between ca. 37°S and 44°S (Luebert and Pliscoff, 2022). Trees such as *Nothofagus obliqua* and *Nothofagus dombeyi* characterize these forests (e.g., Heusser, 2003). These latitudinal changes in plant assemblages align the detection of higher proportions of herbaceous vegetation relative to woody vegetation under dry conditions derived from land cover data by Gaviria-Lugo et al. (2023a). Despite these important changes in plant assemblages, C_4 and CAM plants are only present in minor proportions in the study area (e.g., Arroyo et al., 1990; Powell and Still, 2009; Quezada et al., 2014, 2018) dominated by C_3 plants (Powell and Still, 2009).

Evidence from both simulated and palaeobotanical reconstructions suggest important changes in plant assemblages and plant cover in Chile since the Last Glacial Maximum (e.g., Heusser et al., 2006a, b; Werner et al., 2018). At large temporal and spatial scales the reconstruction of Werner et al. (2018) suggested that the modern plant assemblages detected today along Chile were shifted northward and at lower elevation during the LGM. At smaller temporal and spatial scales, several records indicated episodic changes in vegetation over the last 20 ka BP in Chile (e.g., Heusser et al., 2006b; Jara and Moreno, 2014; Jenny et al., 2002a; Maldonado and Villagrán, 2006; Moreno et al., 2010, 2018; Moreno and Videla, 2016; Muñoz et al., 2020; Pesce and Moreno, 2014; Valero-Garcés et al., 2005; Vargas-Ramirez et al., 2008). These changes, mostly associated with past changes in climate, are discussed further in section 5.3.

2.b.ii A brief discussion of the modern dD isoscape would be useful. Is winter rainfall more deuterium depleted here, like it is in the winter rainfall zone of Southern Africa? It's shown in Fig 2, but it would be nice to have a sentence or two describing the isoscape in the main text as well. Is the predominant rainfall type stratiform or convective? Also what is the average rainfall amount here? What is the predominant driver of the isotopic signal of modern rainfall? Is it rainfall character (stratiform vs convective), is it rainfall amount, vapor source, all the above? Also, do those dD values change during

ENSO or SASM? →Ok, just read further into section 3.6 and see you do address this. So maybe here just include average rainfall amounts in the source area for each site, whether there's a lot of seasonality, and just mention that the controls on rainfall dD will be evaluated in section 5.2?

- **See answer to comment 5.b.ii.**

Methods

3.b.i) RADIOCARBON AGE-DEPTH MODELS Line 226: what do you mean by you 'preferred' the previously published ages?

- The manuscript was reformulated as follows.

Old (Ln 226)	New
We preferred previously published ages acquired on planktic foraminifera samples over benthic foraminifera samples for core sections with a high density of radiocarbon age measurements.	**Note that we preferentially selected** previously published ages acquired on planktic foraminifera samples over benthic foraminifera samples for core sections with a high density of radiocarbon age measurements **(Table 1 reported in Läuchli et al., 2025, see Data availability).**

3.c.i. LIPID EXTRACTION AND N-ALKANE ABUNDANCES Did you calculate Chain-length Preference Index in addition to ACL?

- Carbon Preference Index was added to the manuscript and will be added to the data publication:

[Lines added to Section 3.3 Lipid extraction and *n*-alkane abundances.]	**To evaluate the maturity of the samples and their biological source, we also derived the Carbon Preference Index (CPI) using the concentration of odd- and even-numbered n-alkanes C_{25} to C_{33} following Marzi et al. (1993, Eq. 2).** $$CPI = \frac{(C_{25}+C_{27}+C_{29}+C_{31})+(C_{27}+C_{29}+C_{31}+C_{33})}{2\times(C_{26}+C_{28}+C_{30}+C_{32})} \quad (2)$$
Lines added to **Section 4.2.1 Average chain lengths (ACL) and, abundances of n-alkanes and Carbon Preference Index (CPI)** (renamed).	**The CPI derived at sites GeoB3304-5 and 22SL displayed values ranging between 4.43 and 9.64. These values indicate higher plant-derived long-chain *n*-alkanes (Bush and McInerney, 2013; Eglinton and Hamilton, 1967; Rao et al., 2009).**

3.d.i HYDROGEN AND CARBON ISOTOPIC ANALYSES Why did you choose not to apply a vegetation correction to the dD record? I think skipping the correction is the right move here, especially considering the likely presence of CAM plants, but I think that it's also important to maybe have a sentence just saying "we didn't do this because…"

- The following paragraph was added at the end of Section 3.4.

Added to Section 3.4	Large changes in plant ecophysiology (i.e., C_3, C_4 or CAM pathway plant assemblages) or their water use efficiency can strongly impact δ^2H_{wax} values (e.g., Feakins and Sessions, 2010; Sachse et al., 2006, 2012). Under evidence

	for changes in plant ecophysiology or water use efficiency, a correction on δ^2H_{wax} values is thus needed to derive environmental conditions. Along Chile, no correction was applied to the δ^2H_{wax} values as evidence is lacking for significant changes in plant ecophysiology or their water use efficiency in the study area over the last 20 kyr (see below, Section 5.1).

3.e.i. STATISTICAL METHODS No feedback, though I feel like this section could reasonably be moved to the SI if you need extra room for words. Not sure how strict Climates of the Past is with word-count (honestly, same with much of your methods, you could reasonably move the more detailed descriptions to the SI and just give a brief overview of each section if you need the space).

- The section was kept in the main manuscript as *Climates of the Past* is not strict with word-count. The first two sentences were however deleted as suggested by Anonymous Referee #2.

Results

4.b.i.1. BIOMARKER ANALYSES AVERAGE CHAIN LENGTHS AND ABUNDANCES OF N-ALKANES Can you also list CPI just to verify that the hydrocarbons you are measuring are indeed terrestrial in nature and not petrogenic?

- **See answer to comment *3.c.i.***

4.b.ii. 1 LEAF-WAX N-ALKANE HYDROGEN ISOTOPE RATIOS OF THE MARINE SITES Line 354-356: This sentence doesn't make sense as written, consider rewriting to something like "Although the n-C29 alkane record closely resembles the n-C31 record (see SI fig), we utilize the n-C31 record for further analyses, as it can be directly compared to the n-C31 record of Kaiser et al."

- The manuscript was reformulated as follows:

Old *Line 354-356*	New
The figures showing the n-C29 alkane records – closely resembling the δ2Hwax n-C31 values albeit with overall higher δ2Hwax – are included 355 in the Supplementary Material (Figs. S9 to S13 reported in the Supplementary Material) as not allowing a direct comparison with the δ2Hwax n-C31 record of Kaiser et al. (2024).	**Although the *n*-C_{29} alkane records closely resemble the δ^2H_{wax} *n*-C_{31} values (Figs. S9 and S10 reported in the Supplementary Material), we utilize the δ^2H_{wax} *n*-C_{31} records for further analyses as they can be directly compared to the δ^2H_{wax} *n*-C_{31} record of Kaiser et al. (2024).**

4.b.iii CARBON ISOTOPE RATIOS OF FLUVIAL AND MARINE SEDIMENTS For both carbon and hydrogen, I'd just add a sentence stating that, for modern fluvial and marine samples there is virtually no change in isotopic signal from 42 to ~30 degrees, then the values become progressively enriched as latitude decreases, just to let the reader know that yes, this is something you observed and it will be discussed in the following sections.

- The manuscript was reformulated as follows:

Old (Ln. 363-365)	New
The $\delta^{13}C_{wax}$ of marine surface sediments, corrected for the pre-industrial carbon isotope composition of the atmosphere, ranged from -34 to -29.9‰ (*n*-C_{31}) and -33.6 to -29.3‰ (*n*-C_{29},	The $\delta^{13}C_{wax}$ of marine surface sediments, corrected for the pre-industrial carbon isotope composition of the atmosphere, ranged from -34 to -29.9‰ (*n*-C_{31}) and -33.6 to -29.3‰ (*n*-C_{29},

Fig. 1d, Table S7 in Läuchli et al., 2025, see Data availability).	Fig. 1d, Table **7 reported in** Läuchli et al., 2025, see Data availability). **Note that the modern $\delta^{13}C_{wax}$ values of fluvial and marine surface sediments remain unchanged between 30°S and 42°S, which aligns with the lack of trends detected in the $\delta^{2}H_{wax}$ values between 27°S and 42°S (Gaviria-Lugo et al., 2023a, Fig. 1). Yet, both records display increases north of these latitudes (Fig.1, Sect.5.1, Gaviria-Lugo et al., 2023a)**.

Discussion

5.a.i. CARBON VALUES AS RECORDERS OF PAST CHANGES IN PLANT WATER USE EFFICIENCY ALONG CHILE I feel like an SI figure plotting d13C alongside a few pollen plots from Heusser et al. or Werner et al. could be beneficial to really cement the idea that d13C is capturing water use efficiency and not vegetation change. Really show that, regardless of the vegetation changes observed in the pollen records, water use efficiency is static.

- The following figure was added to the Supplementary material. The figure numbering of the supplementary material was adapted accordingly.

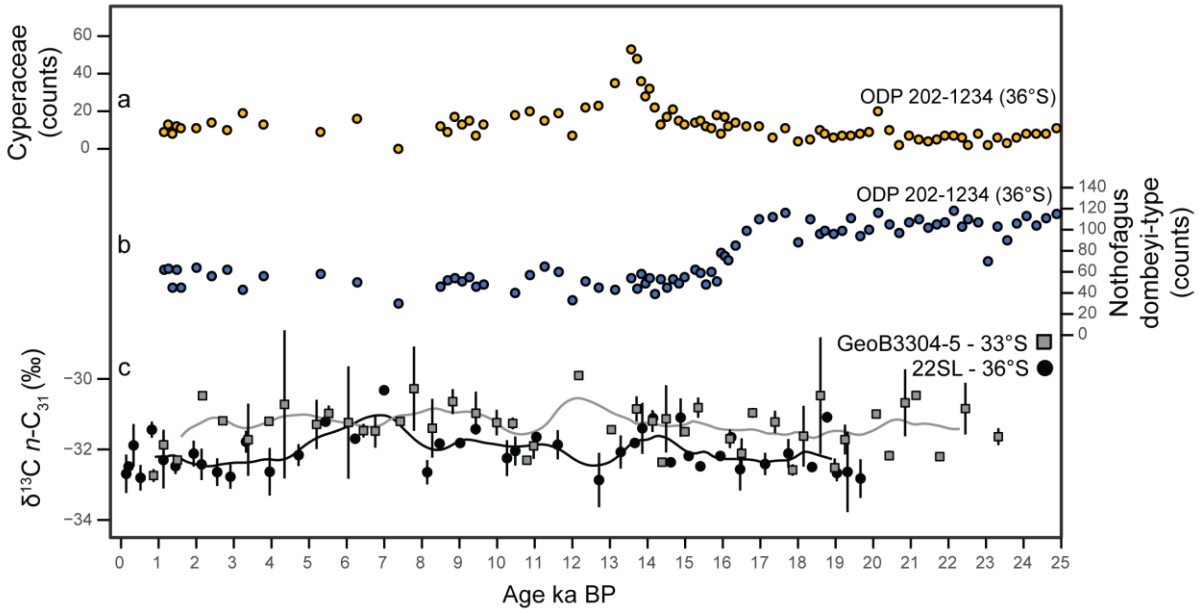

Figure S12. Comparison of the $\delta^{13}C_{wax}$ records of sites GeoB3304-5 and 22SL with pollens records of site ODP 1234 (Heusser et al., 2006a). (a) Cyperaceae counts in site ODP 1234 (36°S) from Heusser et al. (2006a) available under the ACER pollen and charcoal database (ACER project members et al., 2017; Sánchez Goñi et al., 2017) plotted using the age-depth model of Hättig et al. (2023). (b) Nothofagus dombeyi-type counts in site ODP 202-1234 (36°S) from Heusser et al. (2006a) available under the ACER pollen and charcoal database (ACER project members et al., 2017; Sánchez Goñi et al., 2017) plotted using the age-depth model of Hättig et al. (2023). (c) $\delta^{13}C_{wax}$ n-C_{31} records of sites GeoB3304-5 and 22SL. Nothofagus dombeyi-type combines evergreen trees and Cyperaceae is a graminoid family. The lack of relationship between the $\delta^{13}C_{wax}$ record of site 22SL and these pollen records confirm that, despite changes in vegetation, the water use efficiency remains unchanged at the latitude of 33°S and 36°S in Chile over the last 20 kyr.

- Lines 402-404 were modified as follows:

OLD	NEW
The average $\delta^{13}C_{wax}$ values of sites GeoB3304-5 and 22SL remained relatively stable during the last 20 kyr (Fig. 4 and Fig. S11 reported in the Supplementary Material), despite evidence for vegetation changes (e.g., Heusser et al., 2006b; Werner et al., 2018).	The average $\delta^{13}C_{wax}$ values of sites GeoB3304-5 and 22SL remained relatively stable during the last 20 kyr despite evidence for vegetation changes **(Fig. S12 reported in the Supplementary Material, e.g., Heusser et al., 2006b; Werner et al., 2018).**

5.a.ii Line 400: this sentence needs a citation for some paper on d13C in C3 vs C4

- The following references were added:

This low variability in modern δ13Cwax values is consistent with the predominance of C3 pathway plants and/or suggests similar water use efficiency of the different plant assemblages between 30°S and 42°S despite the strong climate gradient of Chile.	This low variability in modern $\delta^{13}C_{wax}$ values is consistent with the predominance of C_3 pathway plants and/or suggests similar water use efficiency of the different plant assemblages between 30°S and 42°S despite the strong climate gradient of Chile **(e.g., Cernusak et al., 2013; Diefendorf and Freimuth, 2017; Kaiser et al., 2008).**

5.b.i LEAF-WAX N-ALKANE HYDROGEN ISOTOPE RATIOS AS A MOISTURE SOURCE PROXY ALONG CHILE Line 420-421: citation needed

- Citation was added:

Old *Line 420-421*	New
As high δ^2H_{wax} values (>ca. -150 ‰) do not occur in the marine archives, we interpret the past δ^2H_{wax} records as past changes in δ^2H_{precip} composition.	As high δ^2H_{wax} values **(>ca. -150 ‰, Gaviria-Lugo et al., 2023a)** do not occur in the marine archives, we interpret the past δ^2H_{wax} records as past changes in δ^2H_{precip} composition.

5.b.ii. *Line 422-425: I'd also cite Aggarwal et al. 2016, as dD values can also be influenced by the proportion of convective vs stratiform rainfall (ie. dD is influenced by vertical motions and microphysical processes within clouds)//* ***2.b.ii*** *A brief discussion of the modern dD isoscape would be useful. Is winter rainfall more deuterium depleted here, like it is in the winter rainfall zone of Southern Africa? It's shown in Fig 2, but it would be nice to have a sentence or two describing the isoscape in the main text as well. Is the predominant rainfall type stratiform or convective? Also what is the average rainfall amount here? What is the predominant driver of the isotopic signal of modern rainfall? Is it rainfall character (stratiform vs convective), is it rainfall amount, vapor source, all the above? Also, do those dD values change during ENSO or SASM? →Ok, just read further into section 3.6 and see you do address this. So maybe here just include average rainfall amounts in the source area for each site, whether there's a lot of seasonality, and just mention that the controls on rainfall dD will be evaluated in section 5.2?* ***5.b.iv.*** *For the section in which you define the four types of dD signals, you mention that north of 27S, annual dD values are governed by SASM precip, is this because of lower rainfall volumes during the rest of the year? Likewise, south of 27S, the annual dD values are dictated by the signal from winter rainfall from the SWW storm track. Again, is this due to extreme seasonality? What is the local phenology like? Do plants in these regions tend to make their waxes at the beginning of the growing season, thus only incorporating the signal from that season? Or do they tend to continuously generate waxes, like grasses do?*

- **The following answer concern comments 2.b.ii, 5.b.ii and 5.b.vi.**
- To respond to the referee comment 2.b.ii, we added a few lines to Section 2.2 regarding the information provided later on in the manuscript.

Old (Ln 159-166)	New
[…]. During the austral summer and autumn, the SWW *core* zone is centered around 50°S and the SWW-driven disturbances (i.e., *peripheral* zone) extend up to ca. 35°S, where they are blocked by the SPH (see above; Strub et al., 1998). During winter, strong precipitation forming the SWW *core* prevails south of 40°S, while the strengthening of the subtropical jet drives the SWW-driven precipitation of the *peripheral* zone northward up to the latitude of 27°S, which corresponds to the southern front of the SPH (Barrett and Hameed, 2017; Flores-Aqueveque et al., 2020; Strub et al., 1998). In contrast to the moisture spells associated with the SPH, the SWW-driven precipitation thus originates from more distant water sources along the storm track. Climate phenomena acting at intra-annual to decadal timescales influence the west coast of South America. […]	[…].During the austral summer and autumn, the SWW *core* zone is centered around 50°S and the SWW-driven disturbances (i.e., *peripheral* zone) extend up to ca. 35°S, where they are blocked by the SPH (see above; Strub et al., 1998). During winter, strong precipitation forming the SWW *core* prevails south of 40°S, while the strengthening of the subtropical jet drives the SWW-driven precipitation of the *peripheral* zone northward up to the latitude of 27°S, which corresponds to the southern front of the SPH (Barrett and Hameed, 2017; Flores-Aqueveque et al., 2020; Strub et al., 1998). **Note that, in contrast to the moisture spells associated with the SPH, the SWW-driven precipitation originates from more distant water sources along the storm track. Overall, these seasonal changes in precipitation amount as well as moisture sources imply changes in the hydrogen isotope signature of precipitation along Chile that are evaluated further in Section 5.2.** **Alongside this seasonal variability,** climate phenomena acting at intra-annual to decadal timescales influence **the clima**te of the west coast of South America. […]

- We also added the MAP values associated with the latitudes of 30°S, 33°S and 36°S to Section 4.2.4 .

Old (Ln. 378-379)	New
The modern mean catchment-averaged temperature and precipitation amounts are reported in Table S8 (Läuchli et al., 2025, see Data Availability).	The modern mean catchment-averaged temperature and precipitation amounts are reported in Table **8 reported in Läuchli et al. (2025, see Data availability). We derived mean annual precipitation amounts of 125 mm/a and 264 mm/a for the Elqui and the Limari river catchments, respectively (ca. 30°S). At ca. 33°S, the mean annual precipitation amounts varied between 344 mm/a in catchment of the Aconcagua River and 564 mm/a in the catchment of the Maipo River. At ca. 36°S, mean annual precipitation amounts of 1015 mm/a and 1245 mm/a were derived for the catchments of the Itata and Biobío rivers, respectively (Table 8 reported in Läuchli et al. 2025, see Data availability).**

- The discussion regarding the role of seasonality was also extended in Section 5.2.

Old (Ln. 437-450)	New
We recognize four distinct δ^2H_{precip} signals along Chile based on the modern catchment-averaged δ2Hprecip values (Figs. 2 and 3). North of 27°S, catchment-averaged δ2Hprecip values more negative than ca. -60‰ (January) are associated with South American Summer Monsoon-driven precipitation (SASM, Figs. 2 and 3, e.g., Garreaud et al., 2009; Vera et al., 2006). Such δ2Hprecip values are consistent with water vapor transport over the Amazonian basin (Fig. 2). Note that north of 27°S, mean annual δ^2H_{precip} values are mainly governed by SASM-driven precipitation. Higher δ2Hprecip values (> -40‰, Figs. 2 and 3) between ca. 27°S and 35°S in January, and north of 27°S in July are consistent with SPH-associated moisture and its more local vapor sources (Sect. 2.2). Further south, SWW-driven precipitation controls δ^2H_{precip} values. Between ca. 45°S and 50°S, values as negative as -100‰ characterize the SWW *core*, while, further north, values around -60‰ characterize the *peripheral* zone of the SWW belt. Note that SWW-driven precipitation controls mean annual δ^2H_{precip} signals south of 27°S as these values resemble those of July (Fig. 3). Past changes in δ2Hprecip values (and thus δ2Hwax values) at a fixed latitude thus reflect latitudinal migration of these climate features. As SASM-driven precipitation are largely limited to north of 27°S	**Different moisture sources affect the Chilean climate (Sect.2). These different moisture sources – evolving at seasonal scale (Sect.2.2) – are associated with distinct δ^2H_{precip} signals, as revealed by the modern catchment-averaged δ^2H_{precip} values along Chile (Figs. 2 and 3).** North of 27°S, catchment-averaged δ^2H_{precip} values more negative than ca. -60‰ (January) are associated with South American Summer Monsoon-driven precipitation (SASM, Figs. 2 and 3, e.g., Garreaud et al., 2009; Vera et al., 2006). Such δ^2H_{precip} values are consistent with water vapor transport over the Amazonian basin (Fig. 2). Note that north of 27°S, mean annual δ^2H_{precip} values are mainly governed by SASM-driven precipitation. **The** higher δ^2H_{precip} values (> -40‰, Figs. 2 and 3) between ca. 27°S and 35°S in January, and north of 27°S in July are consistent with SPH-associated moisture and its more local vapor sources (Sect. 2.2). Further south, SWW-driven precipitation controls δ^2H_{precip} values. Between ca. 45°S and 50°S, values as negative as -100‰ characterize the SWW *core*, while, further north, values around -60‰ characterize the *peripheral* zone of the SWW belt. Note that SWW-driven precipitation controls mean annual δ^2H_{precip} signals south of 27°S as these values resemble those of July (Fig. 3). **This dominant influence of the SWW belt**

on the windward side of the Andes by the topographic barrier associated with the Arid Diagonal Zone (Luebert, 2021), we interpret past δ2Hwax records between 30°S and 36°S in terms of precipitation associated with the SPH, the *peripheral* zone of the SWW belt and the SWW *core*.	**on the mean average hydrogen isotope signature of precipitation is associated with the higher precipitation contribution of the SWW belt compared to the SPH characterized dry conditions (Sect. 2). This dominant influence of the SWW belt on δ^2H_{precip} values south of 30°S is furthermore confirmed by the modern δ^2H_{wax} values of fluvial and marine surface sediments. Between latitudes of 30°S and 33°S, plant growing seasons extend throughout most or all of the year (Hajek and Gutiérrez, 1979). We thus interpret the modern δ^2H_{wax} values between 30°S and 33°S as reflecting mean annual δ^2H_{precip} values and, thus, the hydrogen isotope signal of SWW-driven precipitation. At 36°S, the growing season was determined between October and May (Concepción, Hajek and Gutiérrez, 1979), yet the modern δ^2H_{wax} values reported in Gaviria-Lugo et al. (2023a) still aligns with an influence of the SWW belt. This confirms the predominant role of SWW-driven precipitation in setting mean annual δ^2H_{precip} values south of 30°S. Past changes in δ^2H_{precip} values (and thus δ^2H_{wax} values) at a fixed latitude thus reflect mean annual δ^2H_{precip} values and latitudinal migration of the SPH, the SASM and the SWW belt (see above).** As SASM-driven precipitation are largely limited to north of 27°S on the windward side of the Andes by the topographic barrier associated with the Arid Diagonal Zone (Luebert, 2021), we interpret past δ^2H_{wax} records between 30°S and 36°S in terms of precipitation associated with the SPH, the *peripheral* zone of the SWW belt and the SWW *core*.

- We also added Aggarwal et al. 2016 reference to the manuscript and lines discussing the potential influence of precipitation type on the hydrogen isotope signature of precipitation along Chile.

Old *Line 422-425*	New
The main controls on δ^2H_{precip} values are air temperature (itself controlled by latitude and elevation, Bowen et al., 2019; Dansgaard, 1964; Rozanski et al., 1993), rainfall amount in tropical regions (Bowen et al., 2019; Dansgaard, 1964), continental re-evaporation (Bowen et al., 2019; Salati et al., 1979) and/or the moisture source region and vapor transport (Bailey et al., 2018; Bowen et al., 2019; Putman et al., 2017; Tian et al., 2007).	The main controls on δ^2H_{precip} values are air temperature (itself controlled by latitude and elevation, Bowen et al., 2019; Dansgaard, 1964; Rozanski et al., 1993), rainfall amount in tropical regions (Bowen et al., 2019; Dansgaard, 1964), continental re-evaporation (Bowen et al., 2019; Salati et al., 1979), **precipitation type (convective or stratiform precipitation, Aggarwal et al., 2016)** and/or the moisture source region and vapor transport (Bailey et al., 2018; Bowen et al., 2019; Putman et al., 2017; Tian et al., 2007).

This secondary role of temperature is confirmed by the divergent response of past δ2Hwax records (sites GeoB3304-5 and 22SL) to similar changes in sea surface temperature (ca. 4°C between 17 and 11 ka BP) at 30°S (SST, UK'37 Index, site GeoB7139-2, Kaiser et al., 2008, 435 2024) and 36°S (SST, UK'37 Index, site ODP202-1234, de Bar et al., 2018a, Fig. 5). By a process of elimination, we thus consider δ2Hwax ratios mostly controlled by moisture source origin and vapor transport.	This secondary role of temperature is confirmed by the divergent response **of the GeoB3304-5 and 22SL δ^2H_{wax} records to a ca. 4°C increase in sea surface temperature observed in the alkenone SST records (UK'37 Index) from nearby sites at 30°S (Fig. 5i, Kaiser et al., 2008, 2024) and 36°S** (Fig. 5j, de Bar et al., 2018)**. In addition, we consider a change in precipitation type unlikely to explain changes in the δ^2H_{precip} along Chile as modern precipitation associated with both the SPH and the SWW belt is predominantly stratiform (Viale et al., 2019).** By a process of elimination, we thus consider δ^2H_{precip} values (and thus δ^2H_{wax} ratios) mostly controlled by moisture source origin and vapor transport.

5.b.iii Line 432-435: I'm not sure what the in-text citation style of Climates of the Past dictates (maybe you have to cite the SST records this way, if so ignore this comment). The citations and various parentheses in this sentence make it difficult to figure out. I'd consider rewording it to something like "This secondary role of temperature is confirmed by the opposing responses of the GeoB3304-5 and 22SL dD records to a ~4C increase in temperature observed in the alkenone sst records from nearby sediment cores located at 30S (Fig 5i; Kaiser et al., 2008) and at 36S (Fig 5j; de Bar et al., 2018a)."

- The manuscript was reformulated as follows:

Old *Line 432-435*	New
This secondary role of temperature is confirmed by the divergent response of past δ2Hwax records (sites GeoB3304-5 and 22SL) to similar changes in sea surface temperature (ca. 4°C between 17 and 11 ka BP) at 30°S (SST, UK'37 Index, site GeoB7139-2, Kaiser et al., 2008, 435 2024) and 36°S (SST, UK'37 Index, site ODP202-1234, de Bar et al., 2018a, Fig. 5).	This secondary role of temperature is confirmed by the divergent **response of the GeoB3304-5 and 22SL δ^2H_{wax} records to a ca. 4°C increase in sea surface temperature observed in the alkenone SST records (UK'37 Index) from nearby sites at 30°S (Fig. 5i, Kaiser et al., 2008, 2024) and 36°S** (Fig. 5j, de Bar et al., 2018)**.**

5.b.iv. For the section in which you define the four types of dD signals, you mention that north of 27S, annual dD values are governed by SASM precip, is this because of lower rainfall volumes during the rest of the year? Likewise, south of 27S, the annual dD values are dictated by the signal from winter rainfall from the SWW storm track. Again, is this due to extreme seasonality? What is the local phenology like? Do plants in these regions tend to make their waxes at the beginning of the growing season, thus only incorporating the signal from that season? Or do they tend to continuously generate waxes, like grasses do?

- **See answer to comment 5.b.ii**

5.c.i PAST HYDROLOGICAL REGIME IN CENTRAL CHILE Line 468: "which we attribute to the larger source area"- see my note about figure 1 below.

- **See answer to comment 2.a.iii**. The line was modified as follow:

Old *Line 468:*	New
These δ^2H_{wax} records exhibit considerable scatter, which we attribute to the larger source area at this site compared to sites further north.	These δ^2H_{wax} records exhibit considerable scatter, which we attribute to the larger source area at this site compared to sites further north **(Fig. S2 in Supplementary Material)**.

5.c.ii Lines 485-486: "It also agrees with the wax ratios of site GeoB7139…" – Specify that you mean the 33S and 30S sites more closely agree with one another after 17ka. Right now, it reads as though you're saying the wax record from 33S agrees with the records from both 30S and 36S before 17ka. I'd consider rewording to combine these two sentences into something like: "At 33S, wax values indicate influences of both SWW and SHP over the last 20ka, with lower values prior to 17ka indicating greater influence from SWW core, and higher values after 17ka indicating more of an influence from SWW peripheral. The highest values between 8-5ka suggest influence from the SPH." Then you could say something like, "this coheres with our interpretation of the record from 30S, which indicates influence from the peripheral prior to 17ka and greater influence from the SPH from 14-5ka. Together these records suggest the SWW was in a more northerly position during the LGM"

- At the lines 485-486, our message was that the record from 33°S agrees with the records from both 30°S and 36°S before 17ka in the sense that all records support a northward position of the SWW. The lines were reformulated as follows to make this point clearer:

Old *Lines 485-486*	New
At 33°S (site GeoB3304-5), δ^2H_{wax} values suggest an influence of both the SPH and the SWW belt on local meteoric water composition over the last 20 kyr. Before 17 ka BP, relatively low δ^2H_{wax} values indicate an influence of SWW *core* precipitation that aligns with the values detected further south (see site 22SL). It also agrees with the δ^2H_{wax} ratios (*n*-C31) of site GeoB7139-2 (30°S; Kaiser et al., 2024) indicating an influence the *peripheral* zone of the SWW belt. We thus infer a northern extent of the SWW belt during the LGM (Fig. 4 and Fig. S11 reported in the Supplementary Material). The following increases in δ^2H_{wax} values detected at sites […]	At 33°S (site GeoB3304-5), δ^2H_{wax} values suggest an influence of both the SPH and the SWW belt on local meteoric water composition over the last 20 kyr. Before 17 ka BP, relatively low δ^2H_{wax} values indicate an influence of SWW *core* precipitation that aligns with the values detected further south (see site 22SL). **The records located at 33°S and 36°S thus support a northern position of the SWW belt before 17 ka BP that aligns** with the δ^2H_{wax} ratios (n-C_{31}) of site GeoB7139-2 (30°S; Kaiser et al., 2024) indicating an influence the *peripheral* zone of the SWW belt. We thus infer a northern extent of the SWW belt during the LGM (Fig. 4 and Fig. S11 reported in the Supplementary Material). The **subsequent** increases in δ^2H_{wax} values detected at sites […]

5.c.iv. Line 504-521: I don't feel that this paragraph is absolutely necessary in it's entirety, given that you discuss the phases in detail in the next few subsections. I'd suggest cutting lines 504-510 (the sentences where you discuss the phases) and moving right into timing uncertainties. (something like: "The reconstruction of latitudinal displacement of SWW and SPH- precipitation at 33 and 30S, alongside compiled paleoclimatic records from references 1-15, allow us to define five phases of hydroclimatic regimes. We acknowledge that the precise timing of the transitions between these phases is relatively uncertain due to uncertainties in our age-depth models (4.1), as well as the variability in age constraints in references 1-15, which are generally associated with differences in age-model calibrations, low temporal resolution, variable proxy response times." And then go right into lines 515-521.)

- The paragraph between line 504-521 was rewritten as follows:

Old line 504-521	New
The reconstruction of the latitudinal displacement of SSW- and SPH-driven precipitation at 33°S and 30°S allows defining five time periods, or phases. Phase I (25-17 ka BP) is characterized by an influence of the SWW *core* extending northward to about 33°S. During Phase II (17-14 ka BP), a progressive increase in the δ2Hwax values suggests a southward migration of SWW-driven precipitation. Phase III (14-11.5 ka BP) is defined by a pause in the southward migration of the SWW belt detected at 33°S. The SPH and the SWW belt likely reached their southernmost position during Phase IV (11.5-5.5 ka BP). The Phase IV is subsequently separated in Phase IV A and B as climate changes were detected south of 36°S during this period (Sect. 5.3.4). Phase V (last 5.5 kyr) is marked by a return northward of the influence of the	**The reconstruction of the latitudinal displacement of SSW- and SPH-driven precipitation at 33°S and 30°S, alongside compiled paleoclimatic records summarized in Fig. 4, allows defining five phases of hydroclimatic regimes (see below). We acknowledge that the timings of transitions between these phases are relatively uncertain due to uncertainties in our age-depth models (Sect. 4.1), as well as the variability in age constraints in the different records discussed throughout this work. This variability is generally associated with different age-depth model calibrations (e.g., Lamy et al., 1999), low age-depth model resolutions (e.g., Valero-Garcés et al., 2005) and/or different response times of the proxies used (e.g., Tofelde et al., 2021).**

peripheral zone of the SWW belt up to at least the latitude of 30°S and higher climate variability. Note that relatively high uncertainties are associated with timings of transitions between phases reflecting the uncertainties on the age-depth models (Sect. 4.1). We also acknowledge time lags effects between the different records discussed throughout this work, which we attribute to different age model calibrations (e.g., Lamy et al., 1999), low age model resolutions (e.g., Valero-Garcés et al., 2005), different response times of the proxies used (e.g., Tofelde et al., 2021). The ages determined in this study are thus regarded as broad estimates.	

5.c.v.1+5.v.2 + 5.vi.2 *// 5.v.1: PHASE I Line 541-542: What proxy types support these inferences? / 5.v.2 Same for Line 547-548 / 5.vi.2 Line 560-562: Describe the proxy evidence (I'm not going to comment on this anymore, but throughout this 5.3 I think you need to describe how the proxy evidence supports your inferences. It could be as simple as saying "pollen records from site x indicate vegetation changes consistent with a more mesic environment (citation)." You did well with this in lines 556-560 when you stated that the changes in sedimentology were what suggested the gradual drier conditions.)*

- To answer the referee comments, we included further details regarding the proxies used to reconstruct hydroclimate along Chile. In the main manuscript, we added broad description of the proxies used (see below). In the supplementary material, we added a new table summarizing the method used in each record as well as the coordinated and time range of each record – as suggested by the Anonymous Referee #1. In addition, we extended the Supplementary Texts S1 to S3 to provide further details regarding the proxies used to reconstruct hydroclimate along Chile. A similar paragraph was added to the Supplementary Material (Text S4) for Phase V.
- Below, we show the modification performed to the manuscript and provide the updated Texts S1 to S4, as well as the new Table S1.
- Modification performed to the main article:

Old (Ln. 516-517)	New
The relative changes in the hydrological regimes of each record are summarized in Fig. 4, Figs. S11 and S12 reported in the Supplementary Material.	The relative changes in the hydrological regimes of each record are summarized in Fig. 4 and **Figs. S11, S13 and Table S1 reported in the Supplementary Material.**
PHASE I (Ln. 541-550)	
Lower δ2Hwax values before 17 ka BP imply a more northern position of the SWW *core* than today, with wetter conditions between 33°S and 36°S. Such conditions are consistent with wet and/or cold conditions previously inferred between 30°S and 36°S (Fig. 4, Flores-Aqueveque et al., 2021; Heusser et al., 2006a; Kaiser et al., 2008; Lamy et al., 1999; Valero-Garcés et al., 2005). The detection of slightly higher δ2Hwax values at 30°S (Kaiser et al., 2024) indicating an influence of the *peripheral* zone of the SWW belt, and cold and dry conditions at 31°S (Zech et al., 2007) support reduced precipitation at ca. 30°S compared to the southern latitudes. This indicates an overall northern extent of SWW-driven precipitation during Phase I. Further south, previously published literature also confirm a northern influence of the SWW *core* with cold and wet conditions inferred between 40°S and 46°S (Fig. 4, e.g., Heusser et al., 2006b; Montade et al., 2013; Moreno et al., 2018; Moreno and León, 2003). The lower δ2Hwax values at site OPD1233 (41°S, Kaiser et al., 2024) relative to the δ2Hwax values recorded during the Holocene also implies a northern position of the SWW *core* (i.e., wetter conditions, Kaiser et al., 2024).	Lower δ^2H_{wax} values before 17 ka BP imply a more northern position of the SWW *core* than today, with wetter conditions between 33°S and 36°S. Such conditions are consistent with wet and/or cold conditions previously inferred between 30°S and 36°S **from stratigraphic, sedimentological, geochemical, and palaeobotanical records** distributed onshore and offshore along Chile (Fig. 4, Flores-Aqueveque et al., 2021; Heusser et al., 2006a; Kaiser et al., 2008; Lamy et al., 1999; Valero-Garcés et al., 2005, see Table S1 reported in the Supplementary Material for more details). **In addition, reduced precipitation was inferred at ca. 30°S compared to the southern latitudes by** the detection of slightly higher δ^2H_{wax} values at 30°S (Kaiser et al., 2024) indicating an influence of the *peripheral* zone of the SWW belt, and cold and dry conditions **inferred from past glacier dynamics at 31°S (Zech et al., 2007). Overall, these records confirm** a northern extent of SWW-driven precipitation during Phase I. Further south, previously published literature also confirm a northern influence of the SWW *core* with cold and/or wet conditions inferred between 40°S and 46°S **from palynological and charcoal records, as well as evidence of high runoff in sedimentary records (Fig. 4, e.g.,**

	Heusser et al., 2006b; Montade et al., 2013; Moreno et al., 2018; Moreno and León, 2003, see Table S1 reported in the Supplementary Material for more details). The lower δ^2H_{wax} values at **site ODP 1233** (41°S, Kaiser et al., 2024) relative to the δ^2H_{wax} values recorded during the Holocene also i**mply** a northern position of the SWW *core* (i.e., wetter conditions, Kaiser et al., 2024).
PHASE II	
At 33°S, changes in clay assemblages, grain-sizes and sedimentation rates at the marine sites GIK 17748-2 and GeoB3302 also suggested gradually drier conditions after 18 ka BP (Lamy et al., 1999). At 34.5°S, dry conditions were reconstructed in Laguna Tagua Tagua between 17 and 15 ka BP (Valero-Garcés et al., 2005). At 36°S, a transition toward drier and warmer conditions was also inferred at ca. 17 ka BP (Heusser et al., 2006a; Muratli et al., 2010). (Ln. 558-562)	At 33°S, changes in clay assemblages, grain-sizes and sedimentation rates at the marine sites GIK 17748-2 and GeoB3302 also suggested gradually drier conditions after 18 ka BP (Lamy et al., 1999). At 34.5°S, dry conditions were reconstructed in Laguna Tagua Tagua between 17 and 15 ka BP **from pollen records and $\delta^{18}O$ values** (Valero-Garcés et al., 2005). At 36°S, a transition toward drier and warmer conditions was also inferred at ca. 17 ka **BP from palynological records and change in sediment provenance at site ODP 1234** (Heusser et al., 2006a; Muratli et al., 2010).
Between 36°S and 46°S, the increase in the δ2Hwax values at site OPD1233 (Fig. 5, 41°S, Kaiser et al., 2024), and the detection of drier and warmer conditions between ca. 17.8 ka BP and 14.8 ka BP (e.g., Montade et al., 2013; Moreno et al., 2018; Moreno 570 and León, 2003; Moreno and Videla, 2016; Pesce and Moreno, 2014, further details in Fig. 4, Fig. S12 and Supplementary text S1 in the Supplementary Material) also imply a southward migration (or contraction, Kaiser et al., 2024) of the SWW belt. We also conclude to a southward migration of the southern limit of the SWW *core* between 49°S and 54°S as a transition from dry to wet conditions was detected at ca. 15.9 ka BP at 49°S (Ashworth et al., 1991) and at ca. 15.5 ka BP at 54°S (Heusser et al., 2000). Most records therefore confirm a southward migration of the SWW belt during Phase II. (Ln. 568-574)	Between 36°S and 46°S, the increase in the δ^2H_{wax} values at site **ODP** 1233 (Fig. 5, 41°S, Kaiser et al., 2024), and the detection of drier and warmer conditions between ca. 17.8 ka BP and 14.8 ka BP **from palynological, sedimentary and charcoal evidence** (e.g., Montade et al., 2013; Moreno et al., 2018; Moreno and León, 2003; Moreno and Videla, 2016; Pesce and Moreno, 2014, further details in Fig. 4, Fig. S13 and Supplementary Text S1 in the Supplementary Material) also imply a southward migration (or contraction, Kaiser et al., 2024) of the SWW belt. We **additionally** conclude to a southward migration of the southern limit of the SWW *core* between 49°S and 54°S **as transitions from dry to wet conditions were detected starting at ca. 15.5 ka BP at 49°S and at 54°S in pollen and beetle records** (Ashworth et al., 1991; Heusser et al., 2000). Most records therefore confirm a southward migration of the SWW belt during Phase II.
PHASE III	
Increasing δ2Hwax values in site GeoB7139-2 (Kaiser et al., 2024) and slightly decreasing values in site GeoB3304-5 during Phase III suggest a decoupling of the climate north and south of ca. 32°S. The increasing values at 30°S indicate an increasing influence of the SPH (Kaiser et al., 2024) consistent the drier conditions reconstructed by Bernhardt et al. (2017) and Stuut and Lamy (2004), and the	Increasing δ^2H_{wax} values in site GeoB7139-2 (Kaiser et al., 2024) and slightly decreasing values in site GeoB3304-5 during Phase III suggest a decoupling of the climate north and south of ca. 32°S. The increasing values at 30°S indicate an increasing influence of the SPH (Kaiser et al., 2024) consistent the drier conditions reconstructed **from moisture index records by Bernhardt et al. (2017) and Stuut**

influence of more local moisture spells inferred between 13 and 11.8 ka BP at 31.5°S by Ortega et al. (2012). The decreasing δ2Hwax values at 33°S (GeoB3304-5) instead indicate a return northward of SWW-driven precipitation roughly consistent with the colder and/or wetter conditions reconstructed between 13.5 and 11.5 ka BP in Laguna Tagua Tagua (Valero-Garcés et al., 2005). Most records located between 40°S and 46°S also suggested colder and wetter conditions from ca. 14.8 ka BP and until 12.8 ka BP (e.g., Montade et al., 2013; Moreno et al., 2018; Pesce and Moreno, 2014, Fig. 4, Fig. S12 and Text S2 in the Supplementary Material for further references). (Ln. 576-584)	**and Lamy (2004), and the influence of more local moisture spells inferred from the absence of alluvial deposits between 13 and 11.8 ka BP in peat bog deposits (i.e., relatively high local moisture) located at 31.8°S by Ortega et al. (2012).** The decreasing δ^2H_{wax} values at 33°S (GeoB3304-5) instead indicate a return northward of SWW-driven precipitation roughly consistent with the colder and/or wetter conditions reconstructed **from palynological records at 34.5°S** between 13.5 and 11.5 ka BP **(Laguna Tagua Tagua,** Valero-Garcés et al., 2005). Most palynological, sedimentary and charcoal records located between 40°S and 46°S also suggested colder and wetter conditions from ca. 14.8 ka BP and until **ca**. 12.8 ka BP (e.g., Montade et al., 2013; Moreno et al., 2018; Pesce and Moreno, 2014, Fig. 4, Fig. S13 and Texts S1 and S2 in the Supplementary Material for further references **and detail**s).
During Phase III, we also locate the southern limit of the SWW *core* at around 54°S as relatively wet conditions were detected at ca. 53°C (Fesq-Martin et al., 2004), while a drier interval was suggested between ca. 14.8 and 12.8 ka BP at 54°S (Heusser et al., 2000). Overall, these findings confirm a northward migration of SWW-driven precipitation south of 32°S while progressively drier conditions prevailed north of this latitude between ca. 14 and 12 ka BP. (Ln. 589-593)	During Phase III, we also locate the southern limit of the SWW *core* at around 54°S as relatively wet conditions were detected f**rom palynological records at** ca. 53°C **in a mire** (Fesq-Martin et al., 2004), while a drier interval was suggested **at 54°S** between ca. 14.8 and 12.8 ka BP **by the pollen records of Heusser et al. (2000).** Overall, these findings confirm a northward migration of SWW-driven precipitation south of 32°S while progressively drier conditions prevailed north of this latitude between ca. 14 and 12 ka BP.
PHASE IV	
The high δ2Hwax values of sites GeoB7139-2 and GeoB3304-5 during Phase IV suggest the SPH (i.e., dry conditions) reached latitudes as far south as 33°S (Fig. 4 and Fig. S11 reported in the Supplementary Material). This agrees with the dry and warm conditions previously detected at 30°S (Kaiser et al., 2008; Muñoz et al., 2020, pollen moisture index). Between 32 and 35°S, several records also suggested dry conditions until 5.7 ka BP (Jenny et al., 2002a, 2003; Maldonado and Villagrán, 2006; Valero-Garcés et al., 2005; Villa-Martínez et al., 2003) and 4.2 ka BP (Maldonado and Villagrán, 2002), which confirms a southern extend of the SPH during Phase IV. (Ln 595-600)	The high δ^2H_{wax} values **at** sites GeoB7139-2 and GeoB3304-5 during Phase IV suggest the SPH (i.e., dry conditions) reached latitudes as far south as 33°S (Fig. 4 and Fig. S11 reported in the Supplementary Material). This agrees with the dry and warm conditions previously detected at 30°S **from terrigenous input, sedimentation rates and plant wax n-alkanes records at site GeoB7139-2 (Kaiser et al., 2008) and from pollen moisture index record at the Guanaqueros Bay(30.2°S, Muñoz et al., 2020).** Between 32**°S** and 35°S, **sedimentological records tracing past lake level fluctuations as well as pollen, microfossils (diatoms and microalgae), charcoal and geochemical records also suggested overall dry conditions until ca. 5.7 ka BP** (Jenny et al., 2002a, 2003; Maldonado and Villagrán, 2006; Valero-Garcés et al., 2005; Villa-Martínez et al., 2003) and 4.2 ka BP (Maldonado and Villagrán, 2002, **Table S1 reported in the Supplementary Material**). This

	confirms a southern **extent of** the SPH during Phase IV.
The δ2Hwax values of site GeoB3304-5 (33°S) also showed some lower values between ca. 11 and 7 ka BP. This suggests temporary northward intrusions of SWW-driven precipitation that agrees with the sporadic precipitation events and wetter intervals detected between 11 and 8.5 ka BP from 31°S to 33°S (Jenny et al., 2002a, 2003; Maldonado et al., 2010; Maldonado and Villagrán, 2006; Ortega et al., 2012; Veit, 1996). An increase in the frequency of torrential rainfall was also identified between 8.6 and 6 ka BP in the sedimentological record of the Quebrada Santa Julia archeological site (31.5°S Ortega et al., 2012). This confirms the high sensitivity of site GeoB3304-5 to past δ2Hprecip values. (Ln. 601-606)	The δ^2H_{wax} values **at** site GeoB3304-5 (33°S) also showed some lower values between ca. 11 and 7 ka BP. This suggests temporary northward intrusions of SWW-driven precipitation that agrees with the sporadic precipitation events and wetter intervals detected between 11 and 8.5 ka BP **in several records distributed between 31°S and 33°S in Chile** (Jenny et al., 2002a, 2003; Maldonado et al., 2010; Maldonado and Villagrán, 2006; Ortega et al., 2012; Veit, 1996, **Table S1 reported in Supplementary Material**). **Specifically, evidence for large water level changes at the Laguna Aculeo (34°S) despite overall dry conditions suggests wet intervals between 10 and 9.5 ka BP (Jenny et al., 2002a, 2003). Wetland expansion and evidence for sporadic rainfalls – inferred from pollen records and the presence of alluvial deposits in clayey mud at the Santa Julia archaeological site (31.8°S, Maldonado et al., 2010; Ortega et al., 2012) – also indicated wetter intervals between ca. 10.5 and 8.6 ka BP. This aligns with the reconstruction of a wet phase inferred between ca. 10 and 8.7 ka BP from pollen records at 32.1°S (Maldonado and Villagrán, 2006, swamp forest) and before 7.3 ka BP from geomorphological and pedological evidence found between 27°S and 33°S (Veit, 1996). Note that between 8.6 and 6 ka BP,** an increase in the frequency of torrential rainfall was also identified in the sedimentological record of the Quebrada Santa Julia **archaeological** site (31.5°S Ortega et al., 2012). **These records support temporary northward intrusions of SWW-driven precipitation during Phase IV and confirm** the high sensitivity of site GeoB3304-5 to past δ^2H_{precip} values.
While predominantly dry and warm conditions prevailed north of 36°S, we recognize two distinct climate periods south of 36°S based on previously published literature. Most records between 40°S and 46°S suggested dry and warm conditions until 7.5 ka BP, after which colder and wetter conditions occurred (e.g., Abarzúa et al., 2004; Moreno et al., 2010, 2018; Pesce and Moreno, 2014, see Fig. 4, Fig. S12 and Text S3 in Supplementary Material for further references). This implies a northward migration of the SWW *core* at ca. 7.5 ka BP supported by the lower δ2Hwax values recorded at ca. 8 ka BP in site ODP 1233 (Fig. 5, 41°S, Kaiser et al., 2024). Note	While predominantly dry and warm conditions prevailed north of 36°S, we recognize two distinct climate periods south of 36°S based on previously published literature. Most **palynological, charcoal stratigraphic, sedimentological and geochemical records** between 40°S and 46°S suggested dry and warm conditions until 7.5 ka BP, after which colder and wetter conditions occurred (e.g., Abarzúa et al., 2004; Moreno et al., 2010, 2018; Pesce and Moreno, 2014, see Fig. 4, Fig. S13 and Text S3 in Supplementary Material for further references and details). This implies a northward migration of the SWW *core* at ca. 7.5 ka BP supported by

however that an increase in the δ2Hwax values of site ODP 1233 was then recorded until 5.5 ka BP (Kaiser et al., 2024) suggesting the latitudinal shift of the SWW *core* was only brief. During Phase IV, we locate the southern limit of the SWW *core* south of 56°S between ca. 10 and 7.5 ka BP as suggested by the wet conditions inferred by Perren et al. (2025). After ca. 7.5 ka BP, the SWW *core* likely migrated northward as drier conditions prevailed after 8.5 ka BP between 51°S and 53°S (Lamy et al., 2010) and after 7.5 ka BP at 56°S (Perren et al., 2025). (Ln. 607-615)	the lower δ^2H_{wax} values recorded at ca. 8 ka BP in site ODP 1233 (Fig. 5, 41°S, Kaiser et al., 2024). Note however that an increase in the δ^2H_{wax} values **at** site ODP 1233 was then recorded until 5.5 ka BP (Kaiser et al., 2024) suggesting the latitudinal shift of the SWW *core* was only brief. During Phase IV, we locate the southern limit of the SWW *core* south of 56°S between ca. 10 and 7.5 ka BP as suggested by the wet conditions inferred **from diatoms assemblages and sediment geochemistry at the Isla Hornos Lake** (Perren et al., 2025). After ca. 7.5 ka BP, the SWW *core* likely migrated northward as drier conditions prevailed after 8.5 ka BP **at several sites** between 51°S and 53°S **(Lamy et al., 2010, pollen and sedimentological records**) and after 7.5 ka **BP at the Isla Hornos Lake** at 56°S **(Perren et al., 2025, diatom and geochemical records).**
PHASE V	
Decreasing δ2Hwax values at sites GeoB7139-2 and GeoB3304-5 during Phase V suggest a northward migration of SWW driven precipitation, implying progressively wetter conditions along Chile (Fig. 4 and Fig. S11 reported in the Supplementary Material). This agrees with the wetter conditions reconstructed at the Guanaqueros Bay (30°S) after around 5 ka BP (Muñoz et al., 2020, pollen moisture index) and the gradual increase in humidity reconstructed between ca. 5.7 and 4.2 ka BP at the Palo Colorado swamp forest (32°S; Maldonado and Villagrán, 2006), and between 5.7 and 3.2 ka BP at Laguna Aculeo (33°S; Jenny et al., 2002a; Villa-Martínez et al., 2003). At Laguna Aculeo, higher lake levels were furthermore reconstructed after 6 ka BP (Jenny et al., 2003). A minor change in sediment provenance suggesting a transition toward wetter conditions, and a more variable climate was also detected at around 5 ka BP in the record of site GIK 17748-2 (33°S; Lamy et al., 1999). This contrasts with the record of the Lago Vichuqué at 34.5°S indicating a stronger influence of the SPH between 6.2 and 4 ka BP (Frugone-Álvarez et al., 2017). Yet, as most records suggests an earlier increase in humidity, we consider an onset of the northward migration of SWW-driven precipitation at ca. 5.5 ka BP more likely. (Ln. 621-631)	Decreasing δ^2H_{wax} values at sites GeoB7139-2 and GeoB3304-5 during Phase V suggest a northward migration of SWW-driven precipitation, implying progressively wetter conditions along Chile (Fig. 4 and Fig. S11 reported in the Supplementary Material). This agrees with the wetter conditions reconstructed at the Guanaqueros Bay (30°S) after around 5 ka BP **(Muñoz et al., 2020, pollen moisture index)** and the gradual increase in humidity reconstructed between ca. 5.7 and 4.2 ka **BP from pollen records** at the Palo Colorado swamp forest (32°S; Maldonado and Villagrán, 2006). **An increase in humidity was also inferred between 5.7 and 3.2 ka BP from combined paleoenvironmental tracers at Laguna Aculeo (34°S; Jenny et al., 2002a; Villa-Martínez et al., 2003, Table S1 reported in the Supplementary Material), where** higher lake levels were furthermore reconstructed after 6 ka BP (Jenny et al., 2003). A minor change in sediment provenance suggesting a transition toward wetter conditions, and **more variable** climate **were** also detected at around 5 ka BP at site GIK 17748-2 (33°S; Lamy et al., 1999). This contrasts with **the sedimentological and geochemical records of the Lago Vichuqué (34.5°S) , which indicate** a stronger influence of the SPH between 6.2 and 4 ka BP (Frugone-Álvarez et al., 2017). **Here, we follow the reconstruction supported by most records and determine the onset of the northward migration of SWW-driven precipitation at ca. 5.5 ka BP.**

The high variability of the δ2Hwax *n*-C29 values at site GeoB3304-5 furthermore indicates some climate variability at ca. 4 ka BP, in line with short-term drought and flood events inferred at the Palo Colorado swamp forest after 4.2 ka BP (32°S, Maldonado and Villagrán, 2006) and at Laguna Aculeo after 3 ka BP (33°S, Jenny et al., 2002a, b, 2003; Villa-Martínez et al., 2003, 2004). Similar climate variability was also detected in Southern Chile. (Ln. .632-635)	The high variability of the δ^2H_{wax} *n*-C_{29} values at site GeoB3304-5 furthermore indicates some climate variability at ca. 4 ka BP, in line with short-term drought and flood events inferred from **pollen records** at the Palo Colorado swamp forest after 4.2 ka BP (32°S, Maldonado and Villagrán, 2006) **as well as from combined paleoenvironmental tracers at** Laguna Aculeo after 3 ka BP (34°S, Jenny et al., 2002a, b, 2003; Villa-Martínez et al., 2003, see Table S1 reported in Supplementary Material, 2004). Similar climate variability was also detected in Southern Chile.
Between 40°S and 46°S , the wet conditions inferred at ca 7.5 ka BP persisted over the last 5.5 kyr (Fig. 4, Abarzúa et al., 2004; Haberle and Bennett, 2004; Jara and Moreno, 2014; Montade et al., 2013; Moreno, 2004; Moreno et al., 2010, 2018; Moreno and León, 2003; Pesce and Moreno, 2014; Vargas-Ramirez et al., 2008) and progressively led to modern climate (Haberle and Bennett, 2004; Montade et al., 2013; Moreno et al., 2010). This agrees with the northward expansion of the SWW belt previously suggested by the δ2Hwax record of site ODP1233 (Fig. 5, Kaiser et al., 2024). Superimposed on this progressive increase in precipitation, several records suggested the occurrence of drier (e.g., droughts) and wetter intervals at centennial to millennial timescales (Abarzúa et al., 2004; Haberle and Bennett, 2004; Jara and Moreno, 2012, 2014; Moreno, 2004; Moreno and Videla, 2016; Pesce and Moreno, 2014; Vargas-Ramirez et al., 2008). This confirms an overall high climate variability along Chile during Phase V. (Ln. 636-644)	Between 40°S and 46°S , the wet conditions inferred at ca 7.5 ka BP **from palynological, charcoal stratigraphic, sedimentological and geochemical records distributed onshore and offshore along Chile (Text S3 and Table S1 in Supplementary Material)** persisted over the last 5.5 kyr (Fig. 4, Abarzúa et al., 2004; Haberle and Bennett, 2004; Jara and Moreno, 2014; Montade et al., 2013; Moreno, 2004; Moreno et al., 2010, 2018; Moreno and León, 2003; Pesce and Moreno, 2014; Vargas-Ramirez et al., 2008) and progressively led to modern climate (Haberle and Bennett, 2004; Montade et al., 2013; Moreno et al., 2010). This agrees with the northward expansion of the SWW belt previously suggested by the δ^2H_{wax} record **at** site ODP 1233 (Fig. 5, Kaiser et al., 2024). Superimposed on this progressive increase in precipitation, several records **also** suggested the occurrence of drier (e.g., droughts) and wetter intervals at centennial to millennial timescales (Abarzúa et al., 2004; Haberle and Bennett, 2004; Jara and Moreno, 2012, 2014; Moreno, 2004; Moreno and Videla, 2016; Pesce and Moreno, 2014; Vargas-Ramirez et al., 2008, **Text S4 and Table S1 in Supplementary Material)**. This confirms an overall high climate variability along Chile during Phase V.
During Phase V, we locate the southern limit of the SWW *core* between 53°S and 49°S as dry conditions characterized the last 5.5 ka BP between 51°S and 53°S (Lamy et al., 2010), while a return to wetter conditions was inferred after 3 ka BP at 49°S (Ashworth et al., 1991). Considering these findings, we conclude to a northward migration of SWW-driven precipitation, associated with shorter-term climate variability, as the most likely scenario during Phase V. (Ln. 645-648)	During Phase V, we locate the southern limit of the SWW *core* between 53°S and 49°S as dry conditions **were inferred during** the last 5.5 ka BP between 51°S and 53°S **based on the pollen and sedimentological records of Lamy et al. (2010),** while a return to wetter conditions was **inferred from pollen and fossil beetle assemblages** after 3 ka BP at 49°S (Ashworth et al., 1991). Considering these findings, we conclude to a northward migration of SWW-driven precipitation, associated with shorter-term

	climate variability, as the most likely scenario during Phase V.

- **Updated Texts S1 to S4**

Text S1. Phase II – Paleoclimate conditions

During Phase II, the onset of drier and/or warmer conditions was inferred between 17.8 ka BP and 17 ka BP at sites located south of 40°S. Specifically, this onset was estimated at ca. 17.8 ka BP from lake level lowering and the spread of North Patagonian rainforest at Lago Pichilaguna (41.3°S, Moreno et al., 2018) and the expansion of North Patagonian trees at the Huelmo site (41.5°S, Moreno and León, 2003). Note that overall humid conditions were detected at the Huelmo site until ca. 15.5 ka BP (Moreno and León, 2003). Warmer and/or drier conditions were also inferred at 17.6 ka BP at 46°S from the expansion of Nothofagus woodland reconstructed from the pollen records of the marine site MD07-3088 (Montade et al., 2013). Similar conditions were inferred after 17 ka BP from the pollen records of site ODP 1233 (41°S) and the evidence of the replacement of the North Patagonian and Subantarctic forests and parkland present during the LGM by Valdivian and Lowland Deciduous Forests characteristic of more temperate climate (Heusser et al., 2006b). The end of this overall drier phase was marked by a return to colder and/or wetter conditions detected at 14.8 ka BP from an increase in hygrophilous and cold-tolerant plants at Lago Pichilaguna (41.3°S, Moreno et al., 2018) and the expansion of the conifer Podocarus nubigena at the Huelmo site at 41.5°S (Moreno and León, 2003). On the archipelagos located off the coast of Chile, this transition was dated at 14.7 ka BP from the establishment of forests composed of Nothofagus, Pilgerodendron and Podocarpus trees characteristic of cold and wet conditions detected at the Laguna Facil and the Laguna Oprasa (44°S, Haberle and Bennett, 2004). At the Lago Lepué (42.8°S, Pesce and Moreno, 2014), this return to wetter and/or colder conditions was inferred at 14.6°S from the *Eucryphia*/*Caldcluvia* versus Podocarpaceae (*P. nubigena* and *S. conspicua*) index reflecting hydroclimate variations (ECPI, Moreno, 2004). This transition to wetter conditions was also dated at 14.5 ka BP from an increase in hygrophilous cold resistant trees at the Lago El Salto (41.6°S, Moreno and Videla, 2016) and from evidence for the development of Magellanic moorland in the pollen record at the marine site MD07-3088 (46°S, Montade et al., 2013). Several records located between 40°S and 42°S also inferred this transition at ca. 14 ka BP. These include the pollen records of Heusser et al. (2006b), Jara and Moreno (2014) and Vargas-Ramirez et al. (2008) as well as the ECPI records of Moreno (2004) and Moreno et al. (2010). Note that the record of Murali et al. (2010) suggested an onset of wetter conditions at 15.8 ka BP based on the composition of marine sediments at site ODP 1233 (41°S, Figure S13). Here, we instead refer to the records of Heusser et al. (2006a) and Kaiser et al. (2024) to reconstruct paleoclimate at 41°S since their pollen and δ^2H_{wax} records more directly reflect past hydrological regimes.

Text S2. Phase III – Paleoclimate conditions

Phase III was marked by wet and cold conditions (see Text S1) followed by a transition period until ca. 11.5 ka BP – roughly corresponding to the Younger Dryas (ca. 12.9-11.6 ka BP). The onset of this transition period was dated at 13 ka BP from enhanced fire activity at site Lago El Salto indicting increase precipitation variability and/or seasonality (Moreno and Videla, 2016). A transition period characterized by reduced precipitation was also inferred at 12.8 ka BP from evidence for a retreat of Magellanic moorland in the pollen record at site MD07-3088 (46°S, Montade et al., 2013). A transition period starting at 12.7 ka BP was also detected from pollen and charcoal records suggesting drier conditions at the Lago Pichilaguna (41.3°S, Moreno et al., 2018) and the Lago Lepué (42.8°S, Pesce and Moreno, 2014). Jara and Moreno (2014) used pollen and charcoal records to date the onset of a decrease in precipitation at 12.4 ka BP at Lago Pichilafquén (40.7°S, pollen and charcoal records). In the record of Moreno (2004) and Moreno et al. (2010), we furthermore noted an increase in the ECPI index at around 13 ka BP indicating the onset of a transition to warmer and drier conditions.

These reconstructions suggest a precipitation decrease and/or climate variability during the Younger Dryas.

Overall wet conditions were inferred until between 12.3 ka BP and 11 ka BP after which drier and warmer conditions prevailed. Specifically, the shift to warmer and drier climate was dated at 12.3 ka BP at the Laguna Facil and the Laguna Oprasa (44°S, pollen records, Haberle and Bennett, 2004) and at 12 ka BP based on the pollen records at site ODP 1233, (Heusser et al., 2006b). The onset of a drier period was also dated at 11.6 ka BP in the pollen, charcoal and stratigraphic records of Abarzúa et al. (2004, Laguna Tahui, 42.8°S), the pollen and charcoal records at Lago El Salto (41.6°S, Moreno and Videla, 2016) and the pollen records at Lago Puyehue (40.7°S, Vargas-Ramirez et al., 2008). The pollen and charcoal records at Lago Pichilafquén (40.7°S, Jara and Moreno, 2014), at marine site MD07-3088 (46°S, Montade et al., 2013) and at Lago Condorito (ECPI index, 41.8°S, Moreno, 2004; Moreno et al., 2010) also indicated a transition to drier conditions at 11.5 ka BP. This aligns with the detection of a transition to drier and warmer conditions inferred at 11.3 ka BP at Lago Pichilaguna from the spread of drought-tolerant tree, evidence for low lake level and high frequency of fire activity (Moreno et al., 2018). Furthermore, palynological and stratigraphic changes at the Huelmo site (41.5°S, Moreno and León, 2003) as well as charcoal records and the ECPI index at Lago Lepué (42.8°S, Pesce and Moreno, 2014) confirmed a transition to drier conditions at ca. 11 ka BP. Note that this transition period was not detected in the records of Vargas-Ramirez et al. (2008), Heusser et al. (2006b), Moreno and León (2003), Haberle and Bennet (2004) and Abarzúa et al. (2004). Nevertheless, most reconstructions are consistent with a colder and wetter period between ca. 14 and 12 ka BP and the onset of drier conditions at ca. 11.5 ka BP as suggested by the δ^2H_{wax} records at site GeoB3304-5 at 33°S.

Text S3 Phase IV – Paleoclimate conditions

Most records located between 40°S and 46°S indicated a transition from dry to wet conditions between 8 and 7 ka BP. At 40°S, wetter conditions were detected at 8 ka BP in the pollen records at Lago Puyehue (Vargas-Ramirez et al., 2008) and at 7.1 ka BP in the pollen and charcoal records at Lago Pichilafquén (Jara and Moreno, 2014). Note that the pollen records of Vargas-Ramirez et al. (2008) furthermore suggested an intensification of wetter conditions at 6.8 ka BP. Between 41°S and 44°S, the onset of wetter conditions was dated between 7.9 and 7.6 ka BP (Abarzúa et al., 2004; Moreno, 2004; Moreno et al., 2010, 2018; Moreno and León, 2003; Moreno and Videla, 2016; Pesce and Moreno, 2014). Specifically, wetter conditions were inferred after 7.9 ka BP from palynological and stratigraphical evidence at Laguna Tahui (42.8°S, Abarzúa et al., 2004). At the Lago Condorito (41.8°S), this transition was determined at around 7.6 ka BP based on ECPI record (Text S1, Moreno, 2004; Moreno et al., 2010). At Lago Pichilaguna, wetter conditions were inferred after 7.7 ka BP from stratigraphic pollen and charcoal records (Moreno et al., 2018). Furthermore, palynological and stratigraphic changes at the Huelmo site (41.5°S, Moreno and León, 2003), pollen and charcoal records at Lago El Salto (41.6°S, Moreno and Videla, 2016) as well as charcoal records and the ECPI index at Lago Lepué (42.8°S, Pesce and Moreno, 2014) confirmed a transition to drier conditions between 7.9 and 7.6 ka BP. At 44°S, Haberle and Bennett (2004) suggested seasonally wet conditions between 6.8 and 2.7 ka BP from palynological, geochemical and charcoal records. At 46°S, Montade et al. (2013) dated this transition at 7.4 ka BP using pollen records.

Text S4 Phase V – Paleoclimate conditions

Several records indicated climate variability along Chile during Phase V. At the Laguna Tahui (42.8°S), climate variability was suggested from changes in pollen assemblages after ca. 6.6 ka BP (Abarzúa et al., 2004). At the Laguna Facil and the Laguna Oprasa (44°S), seasonally wet climate was inferred after ca. 6.8 ka BP from palynological evidence and fire records (Haberle and Bennett, 2004). In addition, climate variability potentially related to El-Niño was inferred at these sites after ca. 2.8 ka BP (Haberle and Bennett, 2004). At the Lago Pichilafquén (40.7°S), pollen assemblage shifts and charcoal records also suggested multiple transitions from warm and dry to cold and wet conditions over the last 7.1 ka BP (Jara and Moreno, 2012, 2014). Similarly, dry intervals were detected in the pollen records at the Condorito Lake (41.8°S) between 4.1 and 3.8 ka BP and 2.9 and

1.8 ka BP despite evidence for an overall increase in precipitation between ca. 7 and 3 ka BP (Moreno, 2004). At the Lago El Salto (41.7°S), charcoal and pollen records also indicated alternating cold-wet and warm-dry phases, as well as megadrought events, after 5.3 ka BP (Moreno and Videla, 2016). At the Lago Lepué (42.8°S), dry phases were also inferred from pollen and charcoal records between 4.3 and 4 ka BP and 2 and 0.8 ka BP despite an ECPI index suggesting a sustained shift toward wetter and colder conditions after 7.8 ka BP (Pesce and Moreno, 2014). Dry phases were also inferred at 40.8°S (Lago Puyehue and Los Mallines) from pollen records between 4.6 and 4.3 ka BP and 3 and 2.6 ka BP in the context of overall humid conditions (Vargas-Ramirez et al., 2008).

- Below, we also report Table S1 included in the Supplementary Material.

Table S1

Table S1. Compiled paleoclimatic records in Chile reported in Figure 4d.

#	Ref.	Site	Lat. (WGS 84)	Long. (WGS 84)	Date range of paleoclimate reconstruct. in ka BP	Proxy type tracing paleoclimate conditions
1	Stuut and Lamy, 2004	GeoB3375-1	-27.47	-71.25	35 to 8	Humidity index (grain-size distribution)
2	Muñoz et al., 2020	core BGGC5	-30.2	-71.4	8 to 0	Pollen moisture index
3	Kaiser et al., 2008	GeoB7139-2	-30.20	-71.98	40 to 0	Terrigenous input, sedimentation rates and plant wax n-alkanes
4	Bernhardt et al., 2017	GeoB7139-2	-30.20	-71.98	26 to 0	Humidity index (grain-size distribution)
5	Ortega et al., 2012	Santa Julia archeological site	-31.83	-71.75	13 to 0	Sedimentological and geomorphological
6	Maldonado and Villagrán, 2002	Coastal swamp forest	-31.83	-71.47	6.2 to 0	Palynological
7	Maldonado and Villagrán, 2006	Swamp forest	-32.08	-71.5	10 to 0	Palynological
8	Flores-Aqueveque et al., 2021	Site GNL Quintero 1	-32.77	-71.5	28 to 21	Stratigraphic, sedimentological and geochemical
9	Jenny et al., 2002a	Laguna Aculeo	-33.83	-70.9	10 to 0	Sedimentological, mineralogical, geochemical, palynological and microfossils (diatoms)
10	Jenny et al., 2003	Laguna Aculeo	-33.83	-70.9	10 to 0	Sedimentological
11	Villa-Martínez et al., 2003	Laguna Aculeo	-33.83	-70.9	7.5 to 0	Palynological, charcoal and microalgae records
12	Valero Garcés et al., 2005	Laguna Tagua Tagua	-34.5	-71.1	46 to 6.5	Sedimentological, geochemical and palynological
13	Frugone-Álvarez et al., 2017	Lago Vichuqué	-34.8	-72.05	7 to 0	Sedimentological, geochemical
14	Heusser et al., 2006a	ODP site 202-1234	-36.22	-73.93	140 to 0	Palynological and oxygen isotope ratios records
15	Muratli et al., 2010	ODP site 202-1234	-36.22	-73.93	30 to 0	Petrology/Mineralogy
16	Vargas-Ramirez et al., 2008	Lago Puyehue/ Los Mallines	ca. -40.7	ca. -72.3	17.5 to 0	Palynological
17	Jara and Moreno., 2014	Lago Pichilafquén	-40.73	-72.47	14.5 to 0	Palynological and charcoal record
18	Jara and Moreno, 2012	Lago Pichilafquén	-40.73	-72.47	2.6 to 0	Palynological and charcoal record
19	Heusser et al., 2006b	ODP site 202-1233	-41	-74.45	50 to 9	Palynological
20	Kaiser et al., 2024	ODP site 202-1233	-41	-74.45	50 to 0	Hydrogen isotope on leaf-wax n-alkanes
21	Moreno et al., 2018	Lago Pichilaguna	-41.25	-73.05	25 to 0	Palynological, strati. and charcoal records
22	Moreno and León, 2003	Huelmo site	-41.52	-73	20 to 7	Palynological
23	Moreno and Videla, 2016	Lago El Salto	-41.65	-73.1	16 to 0	Palynological and charcoal record
24	Moreno, 2004	Lago Condorito	-41.75	-73.12	15 to 0	Palynological, ECPI index
25	Moreno et al., 2010	Lago Condorito	-41.75	-73.12	15 to 0	Palynological, ECPI index
26	Pesce and Moreno, 2014	Lago Lepué	-42.8	-73.71	18 to 0	Palynological, ECPI index and charcoal record
27	Abarzúa et al., 2004	Laguna Tahui	-42.83	-73.5	17 to 0	Palynologic and stratigraphic
28	Haberle and Bennett, 2004	Laguna Facil/ Oprasa	ca -44.3	ca.-74	16.5 to 0	Palynological, geochemical and charcoal record
29	Montade et al., 2013	MD07-3088	-46.07	-75.68	22 to 0	Palynological
30	Ashworth et al., 1991	Puerto Edén	-49.13	-74.42	16 to 0	Palynological and beetle fossil record
31	Fesq-Martin et al., 2004	Gran Campo-2	-52.81	-72.93	14 to 5	Palynological
32	Lamy et al., 2010	Several sites	-51°to -53		12.5 to 0	Palynological and sedimentological
33	Heusser et al., 2000	core HE98-1C	-53.61	-70.93	17.6 to 11.5	Palynological
34	Perren et al., 2025	Isla Hornos Lake	-55.97	-67.28	11 ka to 0	Microfossil (diatoms) record and geochemical

5.c.v.3 I'd mention somewhere here that the lack of available data south of 50S and north of ~26S makes determining the full widths of the peripheral and core zones impossible during this phase

- Section 5.3.1 was modified as follows:

Old (Ln- 551-553)	New
Here, we locate the southern limit of the SWW *core* between 46°S and 53°S, as wet conditions were reconstructed at 46°S (Montade et al., 2013) and dry and cold conditions at 53°S (Heusser et al., 2000). This implies a wide SWW *core* extending between 33°S and at least 46°S during Phase I (Fig. 4).	**During this period, the full width of the SWW belt cannot be determined as deciphering Pacific from Atlantic moisture sources in records located north of 26°S (e.g., Betancourt et al., 2000; Latorre et al., 2002, 2006) is difficult without constraints on the past hydrogen isotope composition of precipitation. Furthermore, hydroclimate reconstructions are lacking south of 42°S during this period. At the latitude of 46°S, a pollen record exists, yet this record only informs about paleotemperature (Montade et al., 2013). Further south, at ca. 54°S, the pollen record of Heusser et al. (2000) was used to infer hydroclimate, yet this record only extends until ca. 17.6 ka BP. Nevertheless, the relatively dry conditions inferred before 15.5 ka BP at ca. 54°S imply that the core of the SWW belt was located north of this latitude during Phase I (Fig. 4).**

5.c.vi.1 PHASE II Line 556: I'd add the word "which is" so that this reads "implies a decrease in humidity, which is recognized in…"

Old *Line 556*	New
The southward migration of the SWW belt inferred from the decrease in δ^2H_{wax} records at 30°S and 33°S during Phase II implies a decrease in humidity recognized in most records along Chile.	The southward migration of the SWW belt inferred from **the increase in δ^2H_{wax} values** at 30°S and 33°S during Phase II implies a decrease in humidity**, which is** recognized in most records along Chile.

5.c.vi.3 Line 563: replace "low response" with "minimal response" or "minor response"

Old *Line 563*	New
The low response of site 22SL to the	The **minor** response of site 22SL to the

5.c.iv.4 Line 564-665: and/or suggesting a persistent influence (the way it's written right now sounds like the data scatter could be masking both low amplitude changes and the persistent SWW influence)

- Lines were reformulated as follows:

Old *Line 564-665*	New
The low response of site 22SL to the southward migration of the SWW belt is attributed here to the large scatter of the data, potentially masking low amplitude changes in the δ2Hwax values, and/or a persistent influence of the SWW *core* in the source area of site 22SL. As both hypotheses nevertheless support 565 an	The **minor** response of site 22SL to the southward migration of the SWW belt is attributed here to the large scatter of the data potentially masking low amplitude changes in the δ^2H_{wax} values. **Alternatively, this signal could reflect** a persistent influence of the SWW *core* in the source area of site 22SL. **As these two**

influence of SWW-driven precipitation in the source area of site 22SL during Phase II, we consider a southward migration of the SWW belt as the most likely scenario during this period.	**hypotheses support** an influence of SWW-driven precipitation in the source area of site 22SL during Phase II, we consider a southward migration of the SWW belt as the most likely scenario during this period.

5.c.vii.1 PHASE III Not super critical, but for line 587, when you say the GeoB3304-5 'poorly' cover the time interval, you could include the number of samples or sampling resolution of this interval.

- The sentence was reformulated.

Old *line 587*	New
Such transition period is however not detected in the δ2Hwax records of site GeoB 3304-5 as our records only poorly cover this time interval.	Such transition period is however not detected in the δ^2H_{wax} records at site GeoB 3304-5 as this **time interval is only covered by one sample.**

5.c.viii.1 PHASE IV Line 600: is "extend" supposed to be "extent"?

- Yes.

Old *Line 600*	New
which confirms a southern extend of the SPH during Phase IV.	which confirms a southern extent of the SPH during Phase IV.

5.c.ix.1 PHASE V Line 629: "indicating" should be "which indicates"

Old *Line 629*	New
record of the Lago Vichuqué at 34.5°S indicating a stronger influence of the SPH between	This contrasts **with the sedimentological and geochemical records** of the Lago Vichuqué (34.5°S) , which **indicate** a stronger influence of the SPH between 6.2 and 4 ka BP (Frugone-Álvarez et al., 2017).

5.c.ix.2. Line 630-631: I'd consider rewording this to "While many records suggest an earlier increase in humid conditions, the more negative trend in the wax records from GeoB7139-2 and GeoB3304-5 suggest the northward migration of SWW-precip occurred around 5.5ka"
We initially meant that, as most records indicate an onset of humid conditions at around 5.5 ka BP (including the dD records), we discard the reconstruction of Frugone-Álvarez et al., 2017. To make this clearer, the manuscript was reformulated as follow:

Old *Line 630-631*	New
This contrasts with the record of the Lago Vichuqué at 34.5°S indicating a stronger influence of the SPH between 6.2 and 4 ka BP (Frugone-Álvarez et al., 2017). Yet, as most records suggests an earlier increase in humidity, 630 we consider an onset of the northward migration of SWW-driven precipitation at ca. 5.5 ka BP more likely.	This contrasts with the **sedimentological and geochemical records** of the Lago Vichuqué (34.5°S) , **which indicate** a stronger influence of the SPH between 6.2 and 4 ka BP (Frugone-Álvarez et al., 2017). **Here, we follow the reconstruction supported by most records and determine the onset of the northward migration of SWW-driven precipitation at ca. 5.5 ka BP.**

5.d.i. ATMOSPHERIC PATHWAYS OF THE SOUTH AMERICAN WEST COAST SINCE THE LGM Lines 669-671: I'd consider rewording this to something like "ENSO events are the primary mode of modern interannual variability on the west coast of South America (citations), however, other phenomena such as the MJO and PDO can interfere with the atmospheric pathways associated with ENSO (cite)."

- The manuscript was reformulated as follows:

Old *Lines 669-671*	New
As ENSO events are responsible for most of the modern interannual climate variability on the west coast of South America (Garreaud, 2009; Zhang et al., 2022), no details are given on the atmospheric pathways associated with other modern climate phenomena such as the Madden–Julian Oscillation or the Pacific Decadal Oscillation (Reboita et al., 2021; Zhang et al., 2022). Note however that these phenomena can interfere with the atmospheric pathways associated with ENSO (Yuan et al., 2018).	**ENSO events are the primary mode of modern interannual climate variability on the west coast of South America (Garreaud, 2009; Zhang et al., 2022), however, other phenomena such as the Madden–Julian Oscillation or the Pacific Decadal Oscillation (Reboita et al., 2021; Zhang et al., 2022) can interfere with the atmospheric pathways associated with ENSO (Yuan et al., 2018).**

5.d.ii Line 676: add the word "pathways" so that this reads "these pathways tend to be reduced", as written it is unclear what is being reduced.

Old *Line 676*	New
these tend to be reduced	these **pathways** tend to be reduced

5.d.iii Line 691-694: I'd combine these last two sentences into something like "Our approach focuses solely on the influence of the SWW and ITCZ on hydroclimate in Chile, however, as these features are global, we encourage future works which assess and compare our results to climate reconstructions in locations such as Southwestern Africa and Australia, which are influenced by the same features."

Old *Line 691-694:*	New
Note that our approach is based exclusively on the relationship detected between the SWW belt and the ITCZ along the west coast of South America, whereas atmospheric pathways or teleconnections act at a larger scale. Future research should thus focus on investigating the consistency between our reconstruction of atmospheric pathways and climate at other locations.	**Our approach focuses** exclusively on the **influence of the SWW belt and the ITCZ on hydroclimate in Chile. Yet, as these features act at a larger scale, we encourage future research assessing and comparing our results to climate reconstructions at other locations, such as Southwestern Africa or Australia.**

5.d.iv. 1. LAST GLACIAL MAXIMUM: PHASE I Line 702-703: I'd add the phrase "not consistent" so that this reads "such conditions also imply a weaker subtropical jet and southward shift of the SWW belt, which is not consistent with our observations."

Old *Line 702-703*	New
Yet, considering the mechanisms described by Lee et al. (2011), Ceppi et al.(2013) or Chiang et al. (2014), such conditions also imply a weaker subtropical jet and a shift southward of the SWW belt not observed.	Yet, considering the mechanisms described by Lee et al. (2011), Ceppi et al. (2013) or Chiang et al. (2014), such conditions also imply a weaker subtropical jet and a shift southward of the SWW

	belt, **which is not consistent with our observations.**

5.d.iv.2. I'd briefly mention sea ice in this paragraph somewhere. Maybe in line 705 (e.g. "A more northerly position of the SWW belt during the LGM suggests that a mechanism different that those discussed above may have been active during this period. Further in-depth investigation of regional climate during the LGM is needed, particularly to examine the influence of sea ice-wind interactions on regional hydroclimate."

Old (Ln. 740-705)	New
Further in-depth investigation of climate under the conditions of an ice age – not acquired within the scope of this study – are needed to explain the observed conditions.	Further in-depth investigation of climate under the conditions of an ice age – not acquired within the scope of this study – are needed to explain the observed conditions. **Particularly, future research should focus on examining the influence of sea ice-wind interactions on regional hydroclimate.**

5.d.v. DEGLACIATION PERIOD: PHASE II AND III This whole section feels a little redundant and wordy, making it hard to read. I'd try to condense.

Section 5.4.2 was rewritten as follow:

During the deglaciation period (Phase II and III, ca. 17-11.5 ka BP), the climate conditions along the west coast of South America are consistent with the atmospheric pathways described by Lee et al. (2011) and Chiang et al. (2014). Southward shifts of the SWW belt – derived from paleoclimate reconstructions including our δ2H records (see above) – are associated with southward positions of the ITCZ, such as during Phase II (17-14 ka BP, Fig. 5; Arbuszewski et al., 2013; Deplazes et al., 2013; Yuan et al., 2023), roughly corresponding to the Heinrich Stadial I (HS 1, ca. 18-14.7 ka BP, Naughton et al., 2023) or the Younger Dryas (YD, 12.9-11.6 ka BP, Fig. 5; Deplazes et al., 2013; Haug et al., 2001). Inversely, northward shifts of the SWW belt are associated with northward shifts of the ITCZ, such as during Phase III (Fig. 5; Deplazes et al., 2013; Pedro et al., 2016; Yuan et al., 2023), which roughly corresponds to the Antarctic Cold Reversal (ACR; 14.7 to 13 ka BP; Pedro et al., 2016). Note that some uncertainties are associated with the conditions reconstructed during the Younger Dryas as high-resolution δ2Hwax records are lacking during this period. The southern latitude of the SWW belt during the Younger Dryas is thus deduced solely from evidence of reduced precipitation between 40°S and 46°S (Montade et al., 2013; e.g., Moreno et al., 2018; Moreno and León, 2003). Nevertheless, the climate conditions of the deglaciation period align with atmospheric pathways associated with large changes in interhemispheric thermal gradients and a modulation of the Hadley cell circulation (e.g., Chiang et al., 2014; Lee et al., 2011). Specifically, during Phase II and the Younger Dryas, southward shifts of the ITCZ likely caused a reduction of the SH Hadley cell in turn weakening the subtropical jet and strengthening the mid-latitude jet (Chiang et al., 2014; Lee et al., 2011; Pedro et al., 2018). During the ACR, the opposite conditions prevail and a decoupling of the climate is detected north and south of 32°S – confirmed at larger scale by Pedro et al. (2016). This decoupling likely resulted from the stronger subsidence of the air masses of the Hadley cell (i.e., a stronger SPH) leading to a stronger subtropical jet and the blocking of the disturbance of the SWW belt south of 32°S. Here, high-resolution reconstructions of regional climate thus helped identifying large-scale circulation pathways resulting from large changes in the interhemispheric thermal gradient.

Consensus exists on the predominant role of the interhemispheric thermal gradient on large-scale oceanic and atmospheric circulation changes during the deglaciation period (Fig. 5, Osman et al., 2021; Shakun et al., 2012). The atmospheric pathways reconstructed during the deglaciation period are consistent with these findings. During Phase II and the Younger Dryas, the southward positions of the ITCZ and the SWW belt are in line with large temperature differences between the hemispheres and a colder NH relative to the SH (Bjerknes, 1964; Osman et al., 2021; Pedro et al., 2018; Schneider et al., 2014; Shakun et al., 2012) resulting from reduced AMOC (Fig. 5, Crowley, 1992; Deplazes et al., 2013; Haug et al., 2001; McManus et al., 2004; Moreno-Chamarro et al., 2019; Pedro et al., 2016, 2018; Pöppelmeier et al., 2023). Inversely, during the Bølling-Allerød interstadial period (or ACR), the northward migration of the ITCZ and the SWW belt are associated with a decrease in interhemispheric thermal gradient caused by the relative warming of the NH compared to the SH (Fig. 5, Deplazes et al., 2013; Osman et al., 2021; Pedro et al., 2016; Shakun et al., 2012; Yuan et al., 2023) resulting from a strengthened AMOC (e.g., McManus et al., 2004; Pöppelmeier et al., 2023). This confirms the influence of the mechanisms described, among others, by Lee et al. (2011) and Chiang et al. (2014) on the climate of the west coast of South America during the deglaciation period.

5.d.vi.1. THE HOLOCENE (PHASE IV A AND B, 11.5-5.5 KA BP AND PHASE V, 5.5 KA BP-PRESENT) You start by saying that the Holocene is characterized by small temperature difference between the hemispheres (among other things), but then in the next sentence you say that summer insolation caused asymmetric warming of the Northern and Southern hemispheres, which contradicts the first sentence. Consider rewriting this paragraph.

- We thank the Referee for pointing out this contradiction. The paragraph was reformulated as follow:

Old (Ln. 742-751)	New
During the Holocene, insolation is considered the main forcing of climate as stable AMOC strength (Lippold et al., 2019; McManus et al., 2004; Pöppelmeier et al., 2023b) stable atmospheric CO2 concentrations (Köhler et al., 2017a; Monnin, 2006), and small temperature difference between the hemispheres characterize this period (Fig. 5; Erb et al., 2022b; Osman et al., 2021; Shakun et al., 2012). Specifically, lower summer insolation is recorded in the SH relative to the NH during the early Holocene (Phase IV A, Fig.. 5, Berger, 1988) likely causing a relative cooling of the SH, whereas the opposite conditions prevail during the late Holocene (Phase V). Furthermore, at the late Holocene, the relative warming of the NH compared to the SH was likely enhanced by the larger proportion of landmasses in the NH compared to the SH, responding faster to temperature changes than oceans (e.g., Byrne and O'Gorman, 2013; Joshi et al., 2008). The transition between these two periods (mid-Holocene, between Phase IV B and V) was characterized by lower seasonality (Berger, 1988). Distinct climate conditions were detected over the Holocene, suggesting different atmospheric pathways marked this epoch.	During the Holocene, insolation is considered the main forcing of climate as stable AMOC strength (Lippold et al., 2019; McManus et al., 2004; Pöppelmeier et al., 2023) **and** stable atmospheric **CO_2 concentrations characterize this period** (Köhler et al., 2017; Monnin, 2006). Specifically, lower summer insolation is recorded in the SH relative to the NH during the early Holocene (Phase IV A, Fig. 5, Berger, 1988) likely causing a relative cooling of the SH, whereas the opposite conditions prevail during the late Holocene (Phase V). Furthermore, at the late Holocene, the relative warming of the NH compared to the SH was likely enhanced by the larger proportion of landmasses in the NH compared to the SH, responding faster to temperature changes than oceans (e.g., Byrne and O'Gorman, 2013; Joshi et al., 2008). The transition between these two periods (mid-Holocene, between Phase IV B and V) was characterized by lower seasonality (Berger, 1988). **The above-mentioned changes in insolation imply changes in the interhemispheric thermal gradient, yet the Holocene is characterized by overall small temperature differences between the hemispheres** (Fig. 5; Erb et al., 2022; Osman et al., 2021; Shakun et al., 2012)**. Some mechanisms, such as atmospheric circulation pathways, therefore likely partly or entirely compensated the insolation effect on the temperature of the hemispheres. Alternatively, the effect of insolation on the interhemispheric thermal gradient was only minor compared to the effect of changes in AMOC strength detected during the deglaciation period.**

5.d.vi.2 *Line 752-753: I'd reword this to something like "The relationship between reconstructed climate conditions (including our dD records) and insolation, and inferred atmospheric pathway clearly indicates that local conditions during Phase IV A and V resemble those seen during modern-day ENSO events. Specifically conditions which resemble La Nina during….//* ***5.d.vi.3*** *I'd make it clear in this section that you're not suggesting that your records are resolving individual ENSO events. Also, are you saying that it was just ENSO-like conditions (i.e. sustained presence of warmer waters in the tropical pacific during Phase V indicates an El Padre-type situation) or are you saying that ENSO events were operating to such a degree that it's obfuscating any other climate signals?*

- **Answer to comments 5.d.vi2 and 5.d.vi.3,**
- **To answer the Referee's comments 5.d.vi2 and 5.d.vi.3,** the second paragraph of Section 5.4.3 was reformulated as follow:

Rewritten paragraph 2, Section 5.4.3 (Ln. 752-766)
During the Holocene, we identify different atmospheric pathways based on the climate conditions reconstructed along the west coast of South America – inferred from paleoenvironmental records and δ^2H records. These pathways align with past changes in insolation. During most of the early and late Holocene (Phase IV A and V), climate conditions resemble those observed during modern-day ENSO events. Specifically, during Phase IV A (11.5-7.5 ka BP), a northward position of the ITCZ (Fig. 5; Arbuszewski et al., 2013; Haug et al., 2001; Koutavas et al., 2006; Reimi and Marcantonio, 2016; Schneider et al., 2014; Yuan et al., 2023) – consistent with lower summer insolation in the SH relative to the NH – is associated with a southward SWW belt (Sect. 5.3.4). These conditions resemble La-Niña events and/or a positive SAM phase also inferred elsewhere in South America during the same period (Carré et al., 2012; Jenny et al., 2002a; Koutavas et al., 2002; Ortega et al., 2012; Vargas et al., 2006). During the last 5.5 ka BP (Phase V, late Holocene), the opposite conditions prevail. The ITCZ was progressively shifted southward (Fig. 5, Haug et al., 2001; Schneider et al., 2014; Yuan et al., 2023), reflecting the progressive increase in summer insolation in the SH relative to the NH, while the SWW belt gradually migrated northward (Sect. 5.3.5). This progressive onset of El-Niño-like conditions (and/or a negative SAM) aligns with previously publish studies (Haug et al., 2001; Jenny et al., 2002a; Lamy et al., 2010; Ortega et al., 2019; Sandweiss et al., 1996; Vargas et al., 2006) and the detection of muted ENSO conditions during the mid-Holocene (ca. 5-3 ka BP, e.g., Chen et al., 2016; Emile-Geay et al., 2016; Koutavas and Joanides, 2012). We thus conclude to a relationship between insolation, atmospheric pathways resembling those of modern ENSO events and regional climate during most of the Holocene. Note that our findings do not resolve individual ENSO events and only inform about atmospheric pathways resembling those associated with modern ENSO events. During modern ENSO events, the position of the ITCZ is for instance determined by changes in the energy balance at the tropics and the ITCZ does not typically migrate to the warmer hemisphere. Further investigations, not performed within the scope of this study, are thus needed to confirm a relationship between the changes in sea surface temperature in the Equatorial Pacific – diagnostic of ENSO events – and the atmospheric pathways detected during the Holocene. Our results nevertheless confirm a predominant role of atmospheric pathways resembling those associated with modern ENSO events during the Holocene. Furthermore, their strong response to past changes in insolation highlights the major role of precession cycles (i.e., insolation, Lamy et al., 2019) in setting circulation regimes, and thus regional climate along the west coast of South America during this period.

- We also reformulated lines 769 and 770 as follows:

Old (ln. 769-770)	New
Both atmospheric pathways associated with ENSO and those resulting from large interhemispheric thermal gradients therefore cannot explain these climate conditions.	Both atmospheric pathways **resembling those associated with** ENSO and those resulting from large interhemispheric thermal gradients therefore cannot explain these climate conditions.

6.a. CONCLUSION Line 798: "Antarctic Cord Reversal" should be "Antarctic Cold Reversal"

Old *Line 798*	New
the Antarctic Cord Reversal,	the Antarctic Co**ld** Reversal,

6.b. I'd rewrite/restructure this first paragraph a bit so that it's basically "our study provides the high-res hydroclimate regime reconstruction. Our results essentially show that dD, along with several other proxy records, can be used to infer the location of the SWW belt, with more negative dD values suggesting wetter conditions and a more northerly position of the SWW, and more positive dD values indicating drying and a more southerly position of the SWW. [go into explanation of circulation regime changes and how each phase is characterized by different circulations]

The first paragraph of the conclusion was rewritten as follow:

This study provides a new, high-resolution reconstruction of past hydrological regimes along Chile over the last 20,000 years, based on δ^2H_{wax} records from marine sediments at key latitudes spanning the interface between the Southern Westerly Wind (SWW) belt and the Subtropical Pacific High (SPH). Our results demonstrate that δ^2H_{wax} records, along with previously published hydroclimate reconstructions, can be used to infer the past location of the SWW belt, with more negative δ^2H_{wax} values suggesting wetter conditions and a more northerly position of the SWW belt and more positive δ^2H_{wax} values indicating drier conditions and a more southerly position of the SWW belt. Specifically, our records suggest that central Chile was marked by wet conditions and a northerly SWW belt during the Last Glacial Maximum, after which increasingly drier conditions linked to a southward migration of the SWW belt marked the deglaciation period. This southward migration was partly interrupted during the Antarctic Cold Reversal. During the early Holocene, the SWW belt and the SPH reached their southernmost latitudes, as suggested by the dry conditions that characterized central Chile at that time. At ca. 7.5 ka BP, a displacement northward of the SWW-*core* was detected from wetter conditions reconstructed south of 36°S. The late Holocene was then marked by a progressive northward shift of the SWW belt inferred from a gradual increase in moisture in central Chile over the last 5.5 kyr. By integrating these new δ^2H_{wax} records with reconstructions of past ITCZ positions, we identify major shifts in circulation regimes.

6.c. One thing I'm missing from this paper is any reason why people outside of the paleoclimatic community should care about this. How would it affect them? I'd basically go the standard route and say that our understanding of past climate can help us predict future climate. 'This paper is particularly relevant because it's showing that large scale circulation changes can have highly localized impacts on regional hydroclimate, as the oceans warm the meridional temp gradient will shift and could produce climate states and mechanisms akin to what we see in our reconstructions of the past, etc.'

Lines were added to the second paragraph of the conclusion.

Old (Ln. 806-813)	New
Our reconstruction, combined with past reconstructions of the ITCZ, allow identifying two dominant atmospheric pathways modulating the climate of the west coast of South America since the LGM. Atmospheric pathways driven by large interhemispheric temperature contrasts and changes in the strength of Hadley cells likely prevailed during the last deglaciation period, while, atmospheric pathways associated with ENSO likely dominated during the Holocene, except between 7.5 and 5.5 ka BP. These shifts correspond to changing dominance of major forcings: Atlantic Meridional Overturning Circulation (AMOC) and hemispheric temperature contrasts during the deglaciation period, and orbital insolation forcing (precession) during most of the Holocene. This work highlights the value of δ^2H_{wax} records for unraveling complex hydroclimate patterns and underscores the need for further constraints on large-scale atmospheric pathways to deconvolve past Earth's climate.	Our reconstruction, combined with past reconstructions of the ITCZ, allow identifying two dominant atmospheric pathways modulating the climate of the west coast of South America since the LGM. Atmospheric pathways driven by large interhemispheric temperature contrasts and changes in the strength of Hadley cells likely prevailed during the last deglaciation period, while, atmospheric pathways **resembling those associated with modern ENSO events** likely dominated during the Holocene, except between 7.5 and 5.5 ka BP. These shifts correspond to changing dominance of major forcings: Atlantic Meridional Overturning Circulation (AMOC) and hemispheric temperature contrasts during the deglaciation period, and orbital insolation forcing (precession) during most of the Holocene. This work highlights the value of δ^2H_{wax} records for unraveling complex hydroclimate patterns. **Furthermore, it underscores the need for further constraints on large-scale atmospheric pathways to deconvolve past Earth's climate and predict future climate changes. This is particularly relevant to predict the future impact of large-scale circulation regimes on regional climate in the context of an increase in interhemispheric temperature differences (Friedman et al., 2013).**

7.a. FIGURES/TABLES: Fig 1: I know this figure has a lot of information on it, but would it be possible to highlight the Maipo and Aconcagua rivers, the Biobio and Itata Rivers, and Elqui and Limari Rivers? Just to show exactly where the sediments from the gravity cores is sourced from? If it's too messy on this map, maybe highlight the relevant basins in Fig S8 and point the reader to that in the main text?

- **See answer to comment 2.a.iii**

7.b. Fig 2: This is a fantastic figure, can you just label the sites just so the reader isn't flipping between fig 1 and fig 2

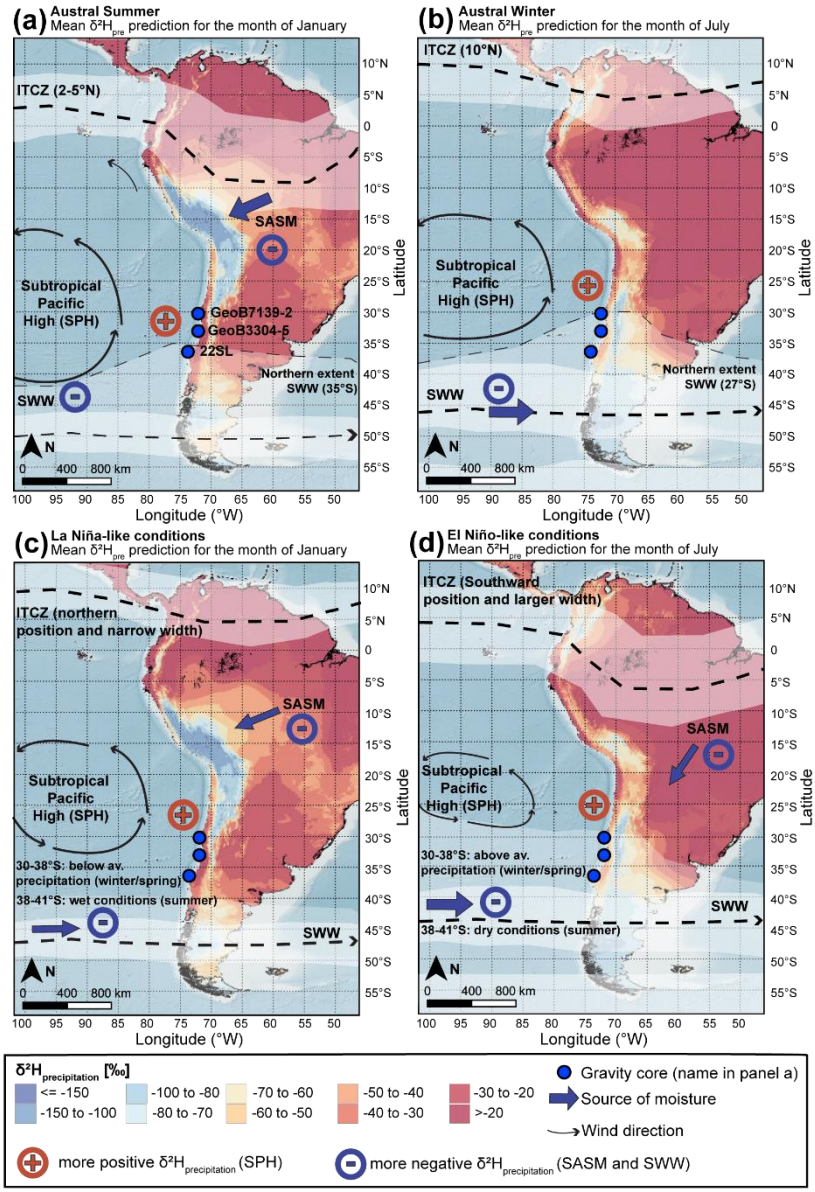

7.c. Fig.3 This is a fantastic figure

7.d. Fig 4: I also really like this figure. The label "Peripherical zone of the SWW belt" could just be "SWW-Peripheral" for consistency. (You'd need to update this in Fig.S11 as well). I suggest that you also make an SI table for the references you use to construct this figure (maybe you've already done this. I'd include the following headings:

Ref no. /name	*Latitude*	*Date Range*	*Proxy Type*

- The label was modified in Fig. 4, S11 and S13 (previously S12) as shown below. A table was also added to the Supplementary Material (Table S1), see answer to comments ***5.c.v.1+5.v.2 + 5.vi.2.***
- Note that the line corresponding to the record of Heusser et al., (2000) was now stopped at 17.6 ka BP. The line corresponding to the record of Moreno and Leon was also stopped at 20 ka BP instead of 25 ka BP. The line corresponding to the record of Pesce and Moreno was also extended to 17.8 ka BP since we now included pollen records (and not only ECPI) as proxies for hydroclimate for this record. These changes do not modify the conclusions associated with this manuscript.

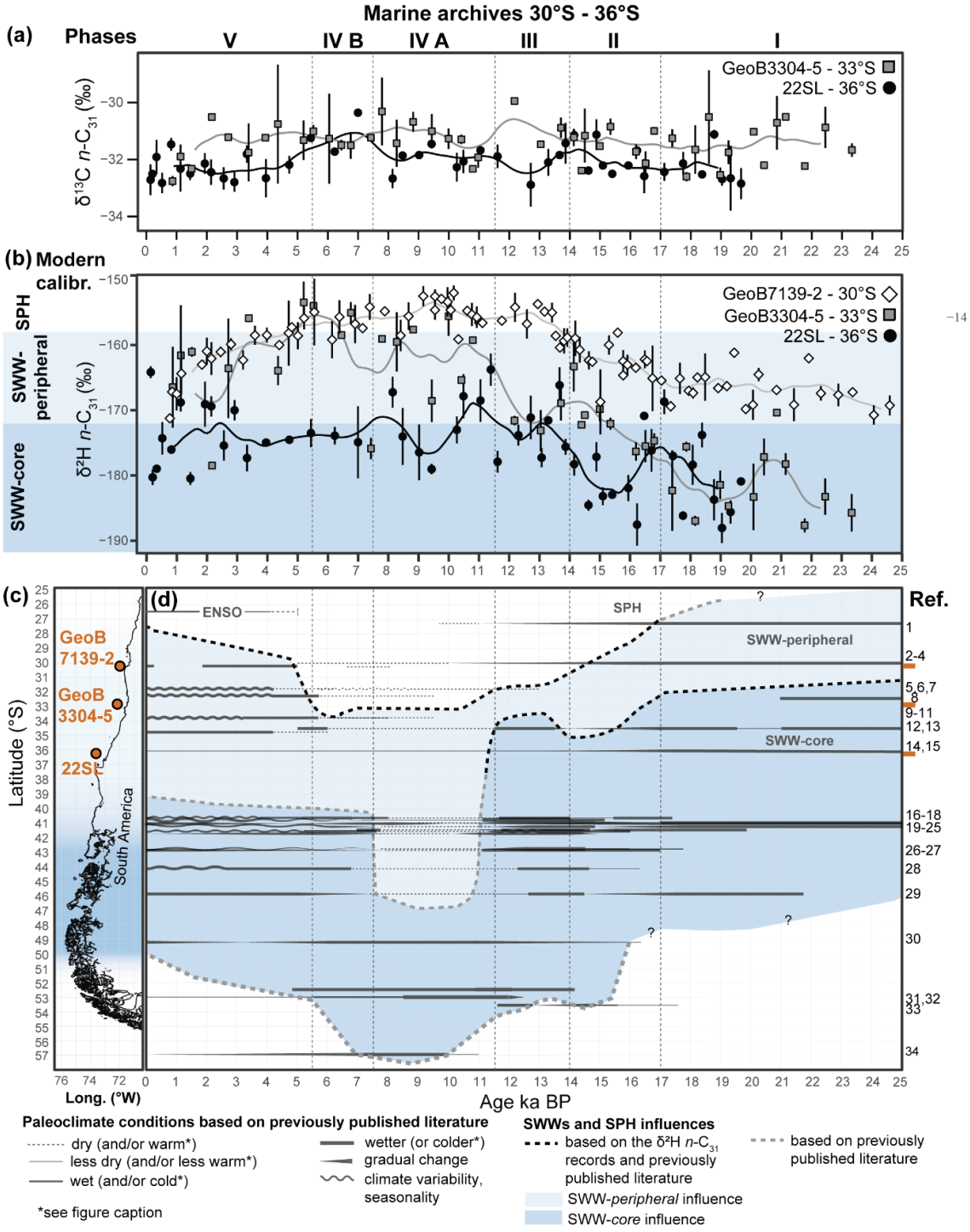

7.e. In both figures 3 and 4 can you mark the timings of Heinrich stadial 1, like you did with the Younger Dryas and Antarctic Cold Reversal?

- The timing of the Heinrich Stadial 1 was added to figures 5 and S14 (previously S13). We did not add this information to Fig. 4 as we consider that this figure already contains enough information. In addition, the above-mentioned periods are only discussed in the context of forcings for the climate exclusively depicted in Figure 5 (and S14 – previously S13).

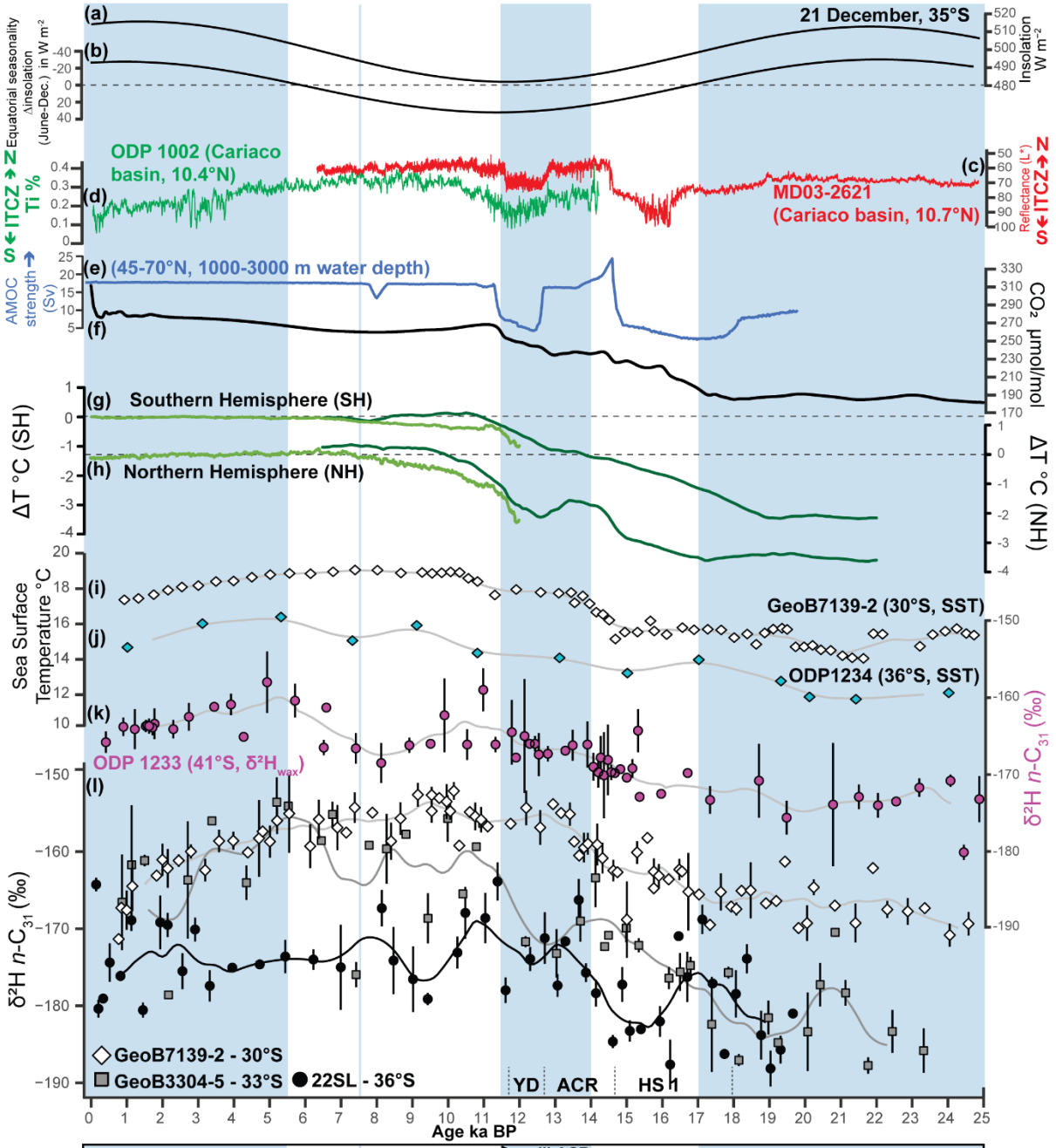

Phase	V	IVB	IVA	III-ACR / III-YD	II - HS 1	I
Age	5 kyr BP - Present	7 - 5 kyr BP	11.5 - 7 kyr BP	14 - 11.5 kyr BP	17 - 14 kyr BP	>17 kyr BP
ITCZ	migration South	North	North	North / South	migr. further South	South of modern position
SWW	migration North	North	South	? / North	migr. further South	North of modern position
Atm. path.	ENSO (El-Niño)	?	ENSO (La-Niña)	ΔT hemisph.	ΔT hemisph.	?

Additional modifications performed on the manuscript:

Lines (in preprint)	*Old*	*New*
45	or the well-studied atmospheric pathways associated with the El Niño-Southern Oscillation (ENSO) phenomenon	or the well-studied atmospheric pathways associated with the ENSO phenomenon
Legend Fig- 3	The more negative δ^2H_{precip} values detected north of 27°S are associated with the South American Summer Monsoon and […]	The more negative δ^2H_{precip} values detected north of 27°S are associated with the South American Summer Monsoon **(SASM)** and […]
395-397	The carbon isotope ratios of leaf-wax *n*-alkanes (expressed as δ13Cwax values) are mainly controlled by plant ecophysiology (i.e., C3 or C4 pathway plant assemblages) and their response to water availability (i.e., water-use efficiency; e.g., Bi et al., 2005; Diefendorf et al., 2015; Liu et al., 2015).	The carbon isotope ratios of leaf-wax *n*-alkanes (expressed as $\delta^{13}C_{wax}$ values) are mainly controlled by plant ecophysiology (i.e., **C_3, C_4 or CAM plants**) and their response to water availability (i.e., water-use efficiency; e.g., Bi et al., 2005; Diefendorf et al., 2015; Liu et al., 2015).
398-399	At present, the latitudes between 26°S and 41°S are characterized by highly heterogenous vegetation, mostly C_3 pathway plants (Powell and Still, 2009, Sect. 2.3),	At present, the latitudes between 26°S and **42°S** are characterized by highly heterogenous vegetation, mostly C_3 pathway plants (Powell and Still, 2009, Sect. 2.3),
474-477	Alternatively, some alteration of δ^2H_{wax} signals before deposition by mixing with the older sediments stored in the Central Valley (Fig. 1; Lowrie and Hey, 1981) could also explain the dispersion of the data at 22SL, yet the clear trends detected in the nearby high-resolution pollen records of site ODP1234 (<1 km, Heusser et al., 2006a) suggest terrestrial signals were not significantly altered before deposition.	Alternatively, some alteration of δ^2H_{wax} signals before deposition by mixing with the older sediments stored in the Central Valley (Fig. 1; Lowrie and Hey, 1981) could also explain the dispersion of the data at 22SL, yet the clear trends detected in the nearby high-resolution pollen records of site **ODP 1234** (<1 km, Heusser et al., 2006a) suggest terrestrial signals were not significantly altered before deposition.
556-559	A gradual decreases in humidity was inferred from the grain-size distributions of site GeoB3375-1 between ca. 17 and 11 ka BP (27°S, Stuut and Lamy, 2004) and of site GeoB7139-2 (30°S) between ca. 16 and 12 ka BP (Bernhardt et al., 2017; recalibrated to the new age-depth model).	A gradual decreases in humidity was inferred **from grai**n-size distributions **at** site GeoB3375-1 between ca. 17 and 11 ka BP (27°S, Stuut and Lamy, 2004) and **at** site GeoB7139-2 (30°S) between ca. 16 and 12 ka BP (Bernhardt et al., 2017; recalibrated to the new age-depth model).
Fig. 4 Caption	**Figure 4** Reconstruction of the past extent of the SWW belt and the SPH based on the hydrogen isotope records of leaf-wax *n*-alkanes (*n*-C31) and previously published literature. (a) δ2Hwax records of sites GeoB7139-2 (30°S, Kaiser et al., 2024), GeoB3304-5 and 22SL (this study). (b) δ13Cwax records of sites GeoB3304-5 and 22SL.	**Figure 1** Reconstruction of the past extent of the SWW belt and the SPH based on the hydrogen isotope records of leaf-wax *n*-alkanes (n-C_{31}) and previously published literature **(a) $\delta^{13}C_{wax}$ records of sites GeoB3304-5 and 22SL. (b) δ^2H_{wax} records of sites GeoB7139-2 (30°S, Kaiser et al., 2024), GeoB3304-5 and 22SL (this study).** (c) Map of the west coast of South America

	(c) Map of the west coast of South America between the 525 latitudes of 25°S and 56°S with the locations of the marine sites. (d) Reconstruction of the past extent of the SWW belt and the SPH. Note the southward migration of the SWW belt at around 17 ka BP, its northward migration during Phase III, its abrupt shift southward during Phase IV and its return northward during Phase V. References: (1) (Stuut and Lamy, 2004), (2) (Muñoz et al., 2020), (3) (Kaiser et al., 2008), (4) (Bernhardt et al., 2017), (5) (Ortega et al., 2012), (6) (Maldonado and Villagrán, 2002), (7) (Maldonado and Villagrán, 2006), (8) (Flores-Aqueveque et al., 2021), (9) (Jenny et al., 2002a), (10) (Jenny et al., 2003), (11) (Villa-Martínez et al., 2003), (12) (Valero-Garcés et al., 2005), (13) (FrugoneÁlvarez et al., 2017), (14) (Heusser et al., 2006a), (15) (Muratli et al., 2010), (16) (Vargas-Ramirez et al., 2008) in which only a cooling was recorded during the ACR, (17) (Jara and Moreno, 2014), (18) (Jara and Moreno, 2012), (19) (Heusser et al., 2006b), (20) (Kaiser et al., 2024), (21) (Moreno et al., 2018), (22) (Moreno and León, 2003), in which only a cooling was recorded during the ACR (23) (Moreno and Videla, 2016), (24) (Moreno, 2004), (25) (Moreno et al., 2010), (26) (Pesce and Moreno, 2014), (27) (Abarzúa et al., 2004), (28) (Haberle and Bennett, 2004), (29) (Montade et al., 2013), (30) (Ashworth et al., 1991), (31) (Fesq-Martin et al., 2004), (32) (Lamy et al., 2010), centered at 53°S, (33) (Heusser et al., 2000), and (34) (Perren et al., 2025). See Sects. 5.3.1 to 5.3.5; Text S1 to S3 and Fig. S12 in the Supplementary Material for details. Error bars correspond to two standard deviations (2σ) calculated from the values reported in the Tables S5 and S6 (Läuchli et al., 2025, see Data availability). The gradient of blue shades in panel C schematically reflects the *core* and *peripheral* zone of the SWW belt as shown in Fig. 3.	between the latitudes of 25°S and 56°S with the locations of the marine sites. (d) Reconstruction of the past extent of the SWW belt and the SPH. Note the southward migration of the SWW belt at around 17 ka BP, its northward migration during Phase III, its abrupt shift southward during Phase IV and its return northward during Phase V. References: (1) (Stuut and Lamy, 2004), (2) (Muñoz et al., 2020), (3) (Kaiser et al., 2008), (4) (Bernhardt et al., 2017), (5) (Ortega et al., 2012), (6) (Maldonado and Villagrán, 2002), (7) (Maldonado and Villagrán, 2006), (8) (Flores-Aqueveque et al., 2021), (9) (Jenny et al., 2002a), (10) (Jenny et al., 2003), (11) (Villa-Martínez et al., 2003), (12) (Valero-Garcés et al., 2005), (13) (Frugone-Álvarez et al., 2017), (14) (Heusser et al., 2006a), (15) (Muratli et al., 2010), (16) (Vargas-Ramirez et al., 2008) in which only a cooling was recorded during the ACR, (17) (Jara and Moreno, 2014), (18) (Jara and Moreno, 2012), (19) (Heusser et al., 2006b), (20) (Kaiser et al., 2024), (21) (Moreno et al., 2018), (22) (Moreno and León, 2003), in which only a cooling was recorded during the ACR (23) (Moreno and Videla, 2016), (24) (Moreno, 2004), (25) (Moreno et al., 2010), (26) (Pesce and Moreno, 2014), (27) (Abarzúa et al., 2004), (28) (Haberle and Bennett, 2004), (29) (Montade et al., 2013) **note that in this record, only cold conditions were inferred before 17.8 ka BP,** (30) (Ashworth et al., 1991), (31) (Fesq-Martin et al., 2004), (32) (Lamy et al., 2010), centered at 53°S, (33) (Heusser et al., 2000), and (34) (Perren et al., 2025). **See Sects. 5.3.1 to 5.3.5; Text S1 to S4 and** Fig. S13 in the Supplementary Material for details. Error bars correspond to two standard deviations (2σ) calculated from the values reported in the Tables 5 and 6 **reported in Läuchli et al. (2025, see Data availability).** The gradient of blue shades in panel C schematically reflects the *core* and *peripheral* zone of the SWW belt as shown in Fig. 3.
Fig. 5 caption	Error bars in (l) represent two standard deviations (2σ) calculated from the values reported in Tables S5 and S6	Error bars in (l) represent two standard deviations (2σ) calculated from the values reported in Tables 5 and 6 reported in Läuchli

	(Läuchli et al., 2025, see Data availability).	et al. (2025, see Data availability). **Abbreviations: ΔT hemisph.: atmospheric pathways driven by large interhemispheric temperature differences; ACR: Antarctic Cold Reversal; YD: Younger Dryas; HS 1: Heinrich Stadial 1.**
Data availability statement	All data generated or analysed during this study (Table S1 to S8) can be found in the following GFZ Data Services repository (Läuchli et al., 2025) […]	All data generated or analysed during this study **(Table 1 to 8)** can be found in the following GFZ Data Services repository (Läuchli et al., 2025) […]